PHILOSOPHICAL TRANSACTIONS OF THE ROYAL SOCIETY A MATHEMATICAL, PHYSICAL & ENGINEERING SCIENCES

Leaky Waves and the Production of Sound by Turbulent Flow from an Elastic Nozzle

M. S. Howe

Phil. Trans. R. Soc. Lond. A 1996 **354**, 1-34
doi: 10.1098/rsta.1996.0001

Leaky waves and the production of sound by turbulent flow from an elastic nozzle

By M. S. Howe

Boston University, College of Engineering, 110 Cummington Street, Boston, MA 02215, USA

An analysis is made of the sound generated by axisymmetric multipole source distributions interacting with the open end of a coaxial nozzle modeled by a semi-infinite circular elastic duct. The influence of surface compliance is important at frequencies below the coincidence frequency ω_c of bending waves on a plate of the same thickness as the duct wall. At frequencies between the ring frequency of the duct, ω_R, and ω_c, the intensity of the sound scattered from the open end is reduced relative to that produced by the same source when the duct is rigid. At lower frequencies, scattering is dominated by sound launched by *leaky* extensional waves of the duct, such that the intensity of the radiation exceeds that from a rigid duct by a factor of order $1/(\kappa_0 a)^2 \gg 1$, where κ_0 and a are, respectively, the acoustic wavenumber and duct radius. The leaky waves propagate supersonically relative to the fluid and cause the radiation directivity to be sharply peaked in an upstream direction determined by the ratio of the sound speed in the fluid and the leaky wave phase velocity. Application of the theory is made to determine the axisymmetric component of the sound produced by low Mach number turbulent flow from the nozzle. Structural compliance would normally be expected to reduce the direct radiation produced by an adjacent turbulent flow, and this is confirmed in the present case at source frequencies between ω_R and ω_c. At lower frequencies, however, the effect is offset by the greater efficiency of leaky wave generation. The net result is that the overall acoustic spectral levels are similar to those for a rigid nozzle, but the directivity is significantly different. Subsonically propagating flexural waves are also generated at the nozzle with an efficiency which, in the case of a steel nozzle in water, exceeds that of sound production via the leaky waves by 30–40 dB at low frequencies. Their influence in the fluid decays rapidly with distance from the nozzle axis, but they may, in practice, make a significant contribution to the flow-generated sound if they are scattered at structural discontinuities upstream of the nozzle exit. The results are illustrated by numerical predictions for a steel nozzle in water. An appendix contains a derivation of a new formula for the sound power radiated by a leaky wave.

Nomenclature

a	radius of cylindrical shell
a_{in}	coefficients in (3.2)
A	$K_0 a$
A_n	constants defined in (2.23)
B	bending stiffness
b_{in}	see (3.3)

Phil. Trans. R. Soc. Lond. A (1996) **354**, 1–34
Printed in Great Britain

B_i	see (2.28)
c	thin-plate extensional wave speed
c_0	speed of sound in the fluid
c_{in}	see (3.6)
C_{ij}	see (2.28)
$D_0(k,\omega)$	dispersion function (2.13) in absence of fluid loading
$D(k,\omega)$	dispersion function, see (2.13)
$\bar{D}(\lambda)$	see (4.11)
E	Young's modulus of material of shell
f	see (2.19)
$\bar{f}$	see (2.14)
$F_\pm$	see (2.30)
G_p	acoustic pressure Green's function
G'_p	free space acoustic pressure Green's function (2.2)
h	thickness of shell
k	wavenumber
K_0	*in vacuo* bending wavenumber $(m\omega^2/B)^{1/4}$
K_η	κ_η/K_0
K_s	κ_s/K_0
ℓ	source length scale
$\ell_\perp$	transverse correlation length, (5.9)
m	mass per unit surface area of shell
M	Mach number
M_c	convection Mach number, $\sim 0.7M$
n_a	see (3.6)
n_ω	see (3.6)
p	time-reduced pressure
p_b	blocked pressure
p_I	incident wave pressure, see (2.3)
p_0	source pressure
p_s	scattered pressure
p'	aerodynamic sound pressure
$P(\lambda)$	see (2.20)
$P'(\lambda)$	$\partial P(\lambda)/\partial\lambda$
P_b	blocked pressure wavenumber–frequency spectrum
r	radial coordinate of cylindrical coordinate system
$\bar{r}$	ring source radius
r_0	ring source radius
R	ring source distance from lip (see figure 2)
$S_n^\pm$	see (2.30)
$T_n^\pm$	see (2.30)
U	mean flow speed
U_c	convection velocity, $\sim 0.7U$
$v_\star$	friction velocity
$W(\lambda)$	see (2.20)
$W_\pm$	see (2.24)
$\bar{W}_+$	see (3.14)
x	axial coordinate
$\bar{x}$	ring source abscissa
X	K_0x
$Z(\lambda)$	see (2.25)
$\mathcal{I}(\lambda)$	$\bar{\mathcal{I}}(\lambda K_0)$
$\bar{\mathcal{I}}(\lambda)$	function defined in (2.11)
$\mathcal{L}$	multipole differential operator
α	c_0/c
α_p	see (5.14)

PHILOSOPHICAL TRANSACTIONS OF THE ROYAL SOCIETY A MATHEMATICAL, PHYSICAL & ENGINEERING SCIENCES

$\gamma(k)$	$(\kappa_0^2 - k^2)^{1/2}$
δ	boundary layer thickness
$\delta_\star$	displacement thickness, $\sim \frac{1}{8}\delta$
ϵ	fluid loading parameter, see (1.2), (2.16)
η	time-reduced complex axial displacement of shell
ζ	time-reduced complex radial displacement of shell
$\zeta_{\rm I}$	see (2.12)
ζ_0	see (2.12)
θ	radiation direction (see figure 2)
Θ	ring source angle (see figure 2)
$\theta_{\rm L}$	leaky wave radiation direction, $\arccos(-\,{\rm Re}\{\kappa_\eta/\kappa_0\})$
$\bar{\theta}$	$\arccos[-\alpha c_{00}\{12/(1-\sigma^2)\}^{1/4}]$
κ	wavenumber
κ_0	acoustic wavenumber, ω/c_0
$\kappa_{\rm R}$	${\rm Re}\{\kappa_\eta\}$
$\kappa_{\rm I}$	${\rm Im}\{\kappa_\eta\}$
κ_η	complex extensional wavenumber on fluid loaded shell
$\kappa_{\rm s}$	subsonic structural wavenumber
λ	k/K_0
λ_j	zero of $P(\lambda)$ in upper half-plane or on positive real axis
Λ	κ/K_0
μ	$(\omega/\omega_{\rm c})^{1/2}$
$\Pi_{\rm A}$	acoustic power
$\Pi_{\rm Ao}$	see (4.15)
$\Pi_{\rm L}$	leaky wave power
Π_0	rigid nozzle acoustic power
$\Pi_{\rm s}$	subsonic structural wave power
Φ	acoustic directivity (4.8)
$\Phi_{\rm pp}$	wall pressure frequency spectrum
Ψ	acoustic pressure spectrum
Ψ_0	rigid nozzle acoustic pressure spectrum
σ	Poisson's ratio
σ_2	$2\epsilon/\mu$
ρ_0	mean fluid density
$\rho_{\rm s}$	density of material of shell
ω	radian frequency
$\omega_{\rm c}$	coincidence frequency
$\omega_{\rm R}$	ring frequency, c/a

1. Introduction

The high-frequency components of the sound produced by a low Mach number turbulent jet tend to be associated primarily with aerodynamic sources near the jet nozzle (see Lilley 1991; Powell 1977*a*, *b*; Ribner 1981, and references cited therein). To make quantitative estimates of the radiation from these sources, it is necessary to include contributions from the unsteady forces exerted on the nozzle by the flow, which are equivalent to dipole sources of sound (Crighton 1991). This can be done explicitly, by first calculating the dipole source strengths, or implicitly by making use of an aeroacoustic Green's function tailored to the appropriate boundary conditions on the nozzle (see, for example, Amiet 1975, 1976, 1986; Cannell 1975, 1976; Cannell & Ffowcs Williams 1973; Crighton 1972*a*, *b*, 1975; Crighton & Leppington 1970, 1971; Ffowcs Williams & Hall 1970; Goldstein 1974; Howe 1975; Kambe *et al.* 1985; Leppington 1971).

Most previous work is concerned with sharp-edged solid boundaries that can be re-

PHILOSOPHICAL TRANSACTIONS OF THE ROYAL SOCIETY A MATHEMATICAL, PHYSICAL & ENGINEERING SCIENCES

garded as *rigid* as far as the production of sound is concerned. Crighton & Leppington (1970), however, have examined the influence of surface compliance for turbulence sources near the edge of a thin elastic plate. They considered the approximation in which the plate is 'locally reacting', which is applicable provided the turbulence length scale is *large* relative to the wavelength of bending waves also excited by the flow, and occurs when the frequency $\omega \ll M^2\omega_c$, where M is the characteristic turbulence Mach number and ω_c is the *coincidence frequency* (above which the phase velocity of bending waves on the plate *in vacuo* exceeds the speed of sound; see Cremer, *et al.* 1988). For a 'limp' plate, the order of magnitude of the ratio Π_A/Π_0 of the acoustic power Π_A to the corresponding power Π_0 generated by the same flow near a *rigid* edge, was found to be given by

$$\frac{\Pi_a}{\Pi_0} = \frac{(\omega/\omega_c)}{\epsilon}, \quad \frac{\omega}{\omega_c} \ll M^2. \tag{1.1}$$

In this expression, ϵ is a fluid loading parameter defined by

$$\epsilon = \rho_0 c_0/m\omega_c, \tag{1.2}$$

where ρ_0, c_0 are, respectively, the fluid density and sound speed, and m is the mass per unit area of the plate (Nayak 1970; Crighton 1988). The estimate (1.1) is valid only for large fluid loading, which occurs typically in underwater applications. For a steel plate in water, for example, $\epsilon \approx 0.135$ and M does not exceed about 0.01; equation (1.1) then indicates that surface compliance greatly reduces the intensity of the sound generated at the edge at very low frequencies. This may be contrasted with the situation in air, where the fluid loading is small ($\epsilon \approx 0.000\,73$ for steel), and the influence of surface compliance on the production of sound is usually negligible, except possibly at high Mach numbers (Maestrello *et al.* 1992). In the higher frequency range, $M^2 \ll \omega/\omega_c < \epsilon^2$, which occurs when the turbulence scale is *small* compared to the bending wavelength, Howe (1993*a*) has shown that (1.1) becomes

$$\Pi_A/\Pi_0 \approx \epsilon(\omega/\epsilon^2\omega_c)^{7/5} < 1,$$

provided the edge of the plate can vibrate freely. More general numerical results given by Howe (1993*b*) indicate that, when fluid loading is large, and at frequencies smaller than the coincidence frequency, the sound radiated directly from the edge is significantly reduced relative to that produced by an identical flow over a rigid edge.

The edge interactions also generate subsonically propagating flexural waves in the plate, that do not radiate energy into the fluid. The flexural wave power is often large, and can exceed the total sound power generated at the edge by 20–40 dB at frequencies $\omega \ll \omega_c$ (and exceed the power radiated by the same flow over a *rigid* edge by 10–20 dB). This suggests that in many practical problems involving high fluid loading, the dominant effective source of sound attributable to a turbulent edge flow may not be the edge, but one or more remote locations where the structure is inhomogeneous or discontinuous and at which structural waves generated at the edge are scattered into sound. The importance of this mechanism of sound generation was first identified by Crighton (1972*c*, 1984).

These conclusions concerning the influence of surface compliance would be expected to be applicable also to sound generated by turbulence in the vicinity of a nozzle lip, provided the acoustic wavelength is much smaller than the nozzle diameter and the frequency is sufficiently high that flexural motions are similar to those on a flat plate. Significant differences may occur at lower frequencies (below the *ring*

PHILOSOPHICAL TRANSACTIONS OF THE ROYAL SOCIETY A MATHEMATICAL, PHYSICAL & ENGINEERING SCIENCES

frequency), however, when the coupling between extensional and radial motions of the nozzle wall becomes important (Lawrie 1986, 1987; Smith 1987; Howe 1993*c*). Extensional waves typically propagate at a supersonic phase velocity (relative to the sound speed in the fluid) and are weakly coupled by surface curvature to radial motions of the wall. This causes the extensional modes to be *leaky*, such that, in the absence of structural damping, all of their energy is ultimately radiated into the fluid as sound. The relatively efficient generation of extensional waves by an edge flow at low frequencies is therefore likely to have a profound effect on the production of sound.

This question is investigated in this paper in terms of an analytical model of turbulent flow at low Mach number from a semi-infinite, circular cylindrical duct. The particular case is considered in which the radiation may be regarded as dominated by the axisymmetric component of the unsteady flow. This approximation is not necessarily valid at higher Mach numbers (Crow & Champagne 1971; Crighton 1972*a*), but the results should be relevant to very low Mach number flows (in water, say) where the fluid loading is large, and where the response of the nozzle to unsteady forcing can be anticipated to have a substantial impact on the generated sound. Attention will be confined to situations in which the phase speed of the extensional waves is supersonic. Then, at very low frequencies it is shown that the dominant component of the scattered sound radiates within a narrow range of directions determined by the leaky waves excited at the nozzle exit. The power radiated by these waves can be calculated by integrating the far field acoustic directivity over a small interval enclosing the leaky wave radiation angle, or by use of a generalization of the usual formula for calculating the power transmitted by a subsonic surface wave, which is derived in the appendix.

The interaction of the flow with the nozzle is formulated as a scattering problem in which the pressure field of the turbulence is scattered at the duct exit. The solution can be expressed in terms of the acoustic pressure Green's function for the semi-infinite elastic cylinder. A general formula for this Green's function is obtained in § 2; in § 3, approximations suitable for applications to aerodynamic sources near the nozzle exit are derived. The general properties of the sound and structural motions produced by a simple time-harmonic edge source are discussed (§ 4), and extension is made to axisymmetric turbulence sources in § 5.

2. Green's function

(*a*) *The governing equations*

Consider an open semi-infinite circular cylindrical elastic duct of radius a and shell thickness $h \ll a$, that occupies, in the undisturbed state, the region $-\infty < x < 0$, $r = a$, of the cylindrical coordinate system (x, r, ϕ) in stationary fluid of mean density ρ_0 and sound speed c_0 (figure 1). Small amplitude motion is excited at time $t = \tau$ by an axisymmetric ring source concentrated on $x = \bar{x}$, $r = \bar{r}$ in the equation for the pressure. The resulting pressure distribution defines the acoustic pressure Green's function, denoted by $G_{\mathrm{p}}(x, \bar{x}, r, \bar{r}, t - \tau)$, where

$$\left(\frac{1}{c_0^2}\frac{\partial^2}{\partial t^2} - \nabla^2\right) G_{\mathrm{p}} = \frac{1}{2\pi r}\delta(x - \bar{x})\delta(r - \bar{r})\delta(t - \tau). \tag{2.1}$$

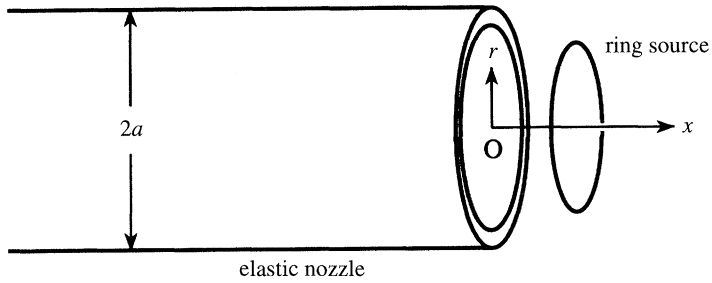

Figure 1. Configuration of the elastic nozzle and ring source.

In the absence of the duct, the solution $G'_{\rm p}$, say, of this equation with outgoing wave behaviour can be expressed as the double Fourier integral (Morse & Ingard 1968)

$$G'_{\rm p}(x,\bar{x},r,\bar{r},t-\tau) = \frac{\mathrm{i}}{16\pi^2} \times \int_{-\infty}^{\infty} (H_0^{(1)}\{\gamma(\kappa)r\}J_0\{\gamma(\kappa)\bar{r}\}H(r-\bar{r}) + J_0\{\gamma(\kappa)r\}H_0^{(1)}\{\gamma(\kappa)\bar{r}\}H(r-\bar{r})) \times \mathrm{e}^{\mathrm{i}\{\kappa(x-\bar{x})-\omega(t-\tau)\}}\,\mathrm{d}\kappa\,\mathrm{d}\omega, \tag{2.2}$$

where J_n and $H_n^{(1)}$ are Bessel and Hankel functions, respectively (Abramowitz & Stegun 1970), $\gamma(\kappa) = (\kappa_0^2 - \kappa^2)^{1/2}$ ($\kappa \equiv \omega/c_0$ being the acoustic wavenumber), with branch cuts defined in the complex κ-plane such that $\gamma(\kappa) = +\mathrm{i}|\gamma(\kappa)|$ for $|\kappa| > |\kappa_0|$ on the real axis, and $H(x)$ is the Heaviside unit function ($= 1, 0$ according as $x \gtrless 0$).

$G_{\rm p}$ may now be determined by considering the scattering by the duct of each wavenumber–frequency component of $G'_{\rm p}$. To fix ideas, we shall assume that $\bar{r} < a$, so that such an incident wavenumber–frequency component can be taken in the form

$$p_{\rm I} = H_0^{(1)}\{\gamma(\kappa)r\}\mathrm{e}^{\mathrm{i}\kappa x}, \quad r > \bar{r}, \tag{2.3}$$

where the harmonic time factor $\mathrm{e}^{-\mathrm{i}\omega t}$ is suppressed and, without loss of generality, it may be assumed that $\omega > 0$ (results for $\omega < 0$ being obtained by analytic continuation in $\mathrm{Im}\,\omega > 0$). If $p_{\rm s}(x,r;\kappa,\omega)$ denotes the corresponding scattered pressure, it then follows from (2.2) that

$$G_{\rm p}(x,\bar{x},r,\bar{r},t-\tau) = G'_{\rm p}(x,\bar{x},r,\bar{r},t-\tau) + \frac{\mathrm{i}}{16\pi^2}\int_{-\infty}^{\infty} p_{\rm s}(x,r;\kappa,\omega)J_0\{\gamma(\kappa)\bar{r}\}\mathrm{e}^{-\mathrm{i}\{\kappa\bar{x}+\omega(t-\tau)\}}\,\mathrm{d}\kappa\,\mathrm{d}\omega, \quad \bar{r} < a. \tag{2.4}$$

The axisymmetric motion produced in the cylinder by the disturbance (2.3) consists of time-harmonic axial and radial displacements, whose complex amplitudes are denoted, respectively, by $\eta(x,r)$ and $\zeta(x,r)$. These displacements are assumed to satisfy the axisymmetric Donnell formulation of the thin shell equations (Cremer *et al.* 1988; Graff 1975; Kraus 1967):

$$\left.\begin{aligned} \left(\frac{\partial^2}{\partial x^2} + \frac{\omega^2}{c^2}\right)\eta + \frac{\sigma}{a}\frac{\partial \zeta}{\partial x} = 0, \\ \left(B\frac{\partial^4}{\partial x^4} - m\omega^2 + m\frac{c^2}{a^2}\right)\zeta + \frac{m\sigma c^2}{a}\frac{\partial \eta}{\partial x} + [p] = 0, \end{aligned}\right\}, \quad x < 0 \tag{2.5}$$

In these equations

$$m = \rho_s h, \quad c = \left(\frac{E}{\rho_s(1-\sigma^2)}\right)^{1/2}, \quad B = \frac{Eh^3}{12(1-\sigma^2)}, \tag{2.6}$$

where ρ_s, E and σ are, respectively, the mass density, Young's modulus and Poisson's ratio of the material of the shell; m is the mass per unit surface area of the shell, and $c\ (> c_0)$ is the phase speed of extensional waves in a thin plate of bending stiffness B. The net pressure force exerted on the shell in the radial direction is equal to $-[p] \equiv -[p_s]$, where $p = p_I + p_s$, and

$$[p_s] = p_s(x, a+0; \kappa, \omega) - p_s(x, a-0; \kappa, \omega). \tag{2.7}$$

The scattered pressure p_s satisfies the time-reduced acoustic equation

$$\frac{1}{r}\frac{\partial}{\partial r}\left(r\frac{\partial p_s}{\partial r}\right) + \frac{\partial^2 p_s}{\partial x^2} + \kappa_0^2 p_s = 0. \tag{2.8}$$

At the surfaces $r = a \pm 0$, $x < 0$ of the duct, ζ and p are also related by the linearized radial component of the fluid momentum equation:

$$\rho_0 \omega^2 \zeta = \frac{\partial p}{\partial r}. \tag{2.9}$$

(*b*) *The edge-scattered field*

The method of solution of the scattering problem is similar to that described by Howe (1993*c*) in considering the interaction of a subsonic flexural wave with the nozzle exit, and only a summary outline of the procedure is necessary here.

The net radial displacement ζ and pressure p can be expressed in the forms

$$\zeta = (\zeta_I + \zeta_0)e^{i\kappa x} + \frac{i\zeta_o}{\kappa_o^2}\int_{-\infty}^{\infty} \gamma(k)\bar{\mathcal{I}}(k)e^{ikx}\,dk, \tag{2.10}$$

$$\frac{p}{\rho_0 c_0^2} = \frac{p_I}{\rho_0 c_0^2} - \frac{\zeta_0 \kappa_0^2 H_0^{(1)}\{\gamma(\kappa)r\}}{\gamma(\kappa) H_1^{(1)}\{\gamma(\kappa)a\}} e^{i\kappa x} - i\zeta_0 \int_{-\infty}^{\infty} \frac{\bar{\mathcal{I}}(k) H_0^{(1)}\{\gamma(k)r\} e^{ikx}}{H_1^{(1)}\{\gamma(k)a\}}\,dk, \quad r > a, \tag{2.11a}$$

$$= \frac{p_I}{\rho_0 c_0^2} - \frac{\zeta_0 \kappa_0^2 J_0\{\gamma(\kappa)r\}}{\gamma(\kappa) J_1\{\gamma(\kappa)a\}} J_1\{\gamma(k)a\} e^{i\kappa x} - i\zeta_0 \int_{-\infty}^{\infty} \frac{\bar{\mathcal{I}}(k) J_0\{\gamma(k)r\} e^{ikx}}{J_1\{\gamma(k)a\}}\,dk, \quad \bar{r} < r < a, \tag{2.11b}$$

for a suitably defined dimensionless function $\bar{\mathcal{I}}(k)$.

In these expressions,

$$\zeta_I = \frac{-\gamma(\kappa) H_1^{(1)}\{\gamma(\kappa)a\}}{\rho_0 \omega^2}, \quad \zeta_0 = \frac{\gamma(\kappa) H_1^{(1)}\{\gamma(\kappa)a\} D_0(\kappa, \omega)}{\rho_0 \omega^2 D(\kappa, \omega)}, \tag{2.12}$$

where

$$\left.\begin{aligned} D_0(k,\omega) &= Bk^4 - m\omega^2 + \frac{mc^2}{a^2} - \frac{m\sigma^2 c^2 k^2}{a^2(k^2-\omega^2/c^2)}, \\ D(k,\omega) &= D_0(k,\omega) - \frac{2\mathrm{i}\rho_0\omega^2}{\gamma(k)\bar{f}\{\gamma(k)a\}}, \end{aligned}\right\} \tag{2.13}$$

and

$$\bar{f}(z) = \pi z J_1(z) H_1^{(1)}(z). \tag{2.14}$$

The integrals in the representations (2.10) and (2.11) account for scattering at the nozzle exit. In (2.10), ζ_{I} is the complex amplitude of the radial displacement of fluid at $r = a$ produced by the incident wave (2.3) when the presence of the duct is ignored (and is expressed in terms of p_{I}, as in equation (2.9)); $\zeta_{\mathrm{I}} + \zeta_0$ is the radial displacement of the shell when scattering at the nozzle exit is ignored, i.e. when the cylinder is assumed to occupy the doubly infinite region $-\infty < x < \infty$. Similarly, in (2.11 *a*) and (2.11 *b*), the second terms on the right-hand sides represent the scattered pressure produced by a doubly infinite cylinder. The formulae (2.10), (2.11) satisfy condition (2.9) at $r = a$, and the Fourier integrals in (2.11) are solutions of the acoustic equation (2.8) with outgoing wave behaviour in $r > a$.

The functions $D(k,\omega)$ and $D_0(k,\omega)$, defined in (2.13), are, respectively, equal to the dispersion functions of axisymmetric flexural waves on an infinite cylinder with, and without, fluid loading. As a function of the wavenumber k, $D(k,\omega)$ has precisely two equal and opposite real zeros $\pm\kappa_{\mathrm{s}}$, say; they satisfy $|\kappa_{\mathrm{s}}| > \kappa_0$ and represent fluid-coupled undamped flexural waves with subsonic phase speeds ($\omega/|\kappa_{\mathrm{s}}| < c_0$). When the fluid loading is large, the most important *complex* zeros of $D(k,\omega)$ occur, respectively, just above and below the real k-axis at $k = \pm\kappa_\eta$, say, where $\mathrm{Re}\{\kappa_\eta\} \approx \omega/c$. These satisfy

$$0 < \mathrm{Im}\{\kappa_\eta\} \ll \mathrm{Re}\{\kappa_\eta\} < \kappa_0,$$

and correspond to *leaky* extensional waves that propagate at phase speeds close to c ($> c_0$) and decay slowly by the radiation of sound into the fluid. Approximate expressions for κ_{s} and κ_η applicable at low frequencies ($\omega a/c \ll 1$, $\omega_{\mathrm{R}} = c/a$) are given in appendix D. For a lightly loaded cylinder (a steel cylinder in air, for example), there can also be a multitude of complex zeros with small imaginary parts that correspond to 'hard-wall' acoustic modes of the duct (see § 3 *e*).

The function $\bar{\mathcal{I}}(k)$ is determined by requiring that (2.10) and (2.11) be consistent with the shell equations (2.5), that the pressure is finite and continuous everywhere, and that appropriate boundary conditions are satisfied at the lip $x = 0$, $r = a$ of the nozzle. The lip is assumed to be free of mechanical constraints, so that the latter conditions are (Kraus 1967)

$$\frac{\partial^2\zeta}{\partial x^2} = 0, \quad \frac{\partial^3\zeta}{\partial x^3} = 0, \quad \frac{\partial\eta}{\partial x} + \frac{\sigma}{a}\zeta = 0, \quad x \to -0. \tag{2.15}$$

(*c*) *Non-dimensional variables*

Further manipulations are simplified by introducing the dimensionless variables,

$$\left.\begin{aligned} &\epsilon = \rho_0\kappa_0/mK_0^2, \quad \mu = \kappa_0/K_0, \quad \sigma_2 = 2\epsilon/\mu, \\ &X = K_0 x, \quad A = K_0 a, \quad \Lambda = \kappa/K_0, \quad K_\eta = \kappa_\eta/K_0, \quad K_{\mathrm{s}} = \kappa_{\mathrm{s}}/K_0. \end{aligned}\right\} \tag{2.16}$$

$K_0 = (m\omega_2/B)^{1/4}$ denotes the bending wavenumber on a flat plate of thickness h in the absence of fluid loading; ϵ is the fluid loading parameter defined in (1.2) in terms

of the *coincidence frequency* $\omega_c = c_0^2(m/B)^{1/2}$; it is also given by

$$\epsilon = \frac{\rho_0}{\rho_s}\left(\frac{E}{12\rho_s c_0^2(1-\sigma^2)}\right)^{1/2} \equiv \frac{1}{\sqrt{12}}\frac{\rho_0 c}{\rho_s c_0}. \tag{2.17}$$

Similarly,

$$\mu = \left(\frac{\omega}{\omega_c}\right)^{1/2}, \quad \frac{\omega_c h}{c_0} = \frac{c_0}{c}\sqrt{12} \equiv \frac{\rho_0}{\epsilon\rho_s}. \tag{2.18}$$

It is also convenient to make the change of variable $k = \lambda K_0$ in the integrals of (2.10), (2.11), and to introduce the following dimensionless functions:

$$f(\lambda) \equiv \bar{f}(\mathrm{i}A\sqrt{\lambda^2-\mu^2}) = 2A\sqrt{\lambda^2-\mu^2}I_1(A\sqrt{\lambda^2-\mu^2})K_1(A\sqrt{\lambda^2-\mu^2}), \tag{2.19}$$

$$\left.\begin{aligned} P(\lambda) &= \frac{(\lambda^2-\alpha^2\mu^2)D_0(\lambda K_0,\omega)}{m\omega^2} \\ &\equiv \{\lambda^2-(\alpha\mu)^2\}\{\lambda^4-1+1/(\alpha\mu A)^2\}-\sigma^2\lambda^2/(\alpha\mu A)^2, \\ W(\lambda) &= \frac{\sqrt{\lambda^2-\mu^2}f(\lambda)(\lambda^2-\alpha^2\mu^2)D(\lambda K_0,\omega)}{m\omega^2} \\ &\equiv \sqrt{\lambda^2-\mu^2}f(\lambda)P(\lambda)-\sigma_2\{\lambda^2-(\alpha\mu)^2\}, \end{aligned}\right\} \tag{2.20}$$

where I_1, K_1 are modified Bessel functions (Abramowitz & Stegun 1970), $\alpha = c_0/c$, and branch cuts of $\sqrt{\lambda^2-\mu^2}$ in the complex λ-plane are taken such that, on the real axis, $\sqrt{\lambda^2-\mu^2}$ is positive for $|\lambda| > \mu$, and negative imaginary for $|\lambda| < \mu$. $P(\lambda)$ is a cubic polynomial in λ^2, whose zeros $\pm\lambda_1$, $\pm\lambda_2$, $\pm\lambda_3$ are equal to the non-dimensional wavenumbers of flexural waves on the cylinder *in the absence of fluid loading*. Two of these, $\pm\lambda_1$, say, are always real and occur near $\lambda = \pm\alpha\mu \approx \pm\mathrm{Re}\{K_\eta\}$; they correspond to extensional waves on the cylinder in the absence of the fluid. Of the remaining roots, $\pm\lambda_2$, say, are real when ω exceeds the ring frequency c/a (when they approximate to the wavenumbers of bending waves on a plate *in vacuo*), whereas the final pair $\pm\lambda_3$ are always complex. To fix the notation, it will be assumed that the roots $+\lambda_1$, $+\lambda_2$, $+\lambda_3$ are either positive and real or have positive imaginary parts. The function $W(\lambda)$ has only two real zeros at $\lambda = \pm K_s$ ($K_s > \mu$), corresponding to the real zeros of the dispersion function $D(k,\omega)$. It also has two complex zeros, $\pm K_\eta$, close to the real λ-axis (near $\pm\lambda_1$), which correspond to the *leaky* extensional modes.

(*d*) *Dual integral equations for* $\bar{\mathcal{I}}(k)$

Eliminate the axial displacement η from equations (2.5) by differentiating the first equation with respect to x and substituting for $\partial\eta/\partial x$ and $\partial^3\eta/\partial x^3$ from the second. The resulting equation must be satisfied by the representations (2.10), (2.11) of ζ and p, and this implies that

$$\int_{-\infty}^{\infty}\frac{W(\lambda)}{f(\lambda)}\mathcal{I}(\lambda)\mathrm{e}^{\mathrm{i}\lambda X}\,\mathrm{d}\lambda = 0, \quad X < 0. \tag{2.21}$$

where $\mathcal{I}(\lambda) \equiv \bar{\mathcal{I}}(\lambda K_0)$.

The pressure p is continuous throughout the fluid provided the representations (2.11 *a*) and (2.11 *b*) are equal on $r = a$, $x > 0$. By making use of the identity $H_0^{(1)}(z)/H_1^{(1)}(z) - J_0(z)/J_1(z) \equiv 2i/\bar{f}(z)$ (Abramowitz & Stegun 1970), this condition

reduces to

$$\int_{-\infty}^{\infty} \frac{\mathcal{I}(\lambda)}{f(\lambda)} e^{i\lambda X}\, d\lambda = \frac{\mu^2 e^{i\Lambda X}}{f(\Lambda)\sqrt{\Lambda^2-\mu^2}}, \quad X>0. \tag{2.22}$$

The solution $\mathcal{I}(\lambda)$ of the dual integral equations (2.21), (2.22) is discussed by Howe (1993*c*), and it is sufficient to write down the particular form that ensures that the pressure loading $-[p_s]$ vanishes at the lip ($x \to -0$):

$$\mathcal{I}(\lambda) = \frac{\mu^2 W_+(\Lambda) f(\lambda)}{2\pi i W_+(\lambda) f(\Lambda)\sqrt{\Lambda^2-\mu^2}} \left[\frac{1}{\lambda-\Lambda-i0} + \sum_{n=0}^{2} A_n \lambda^n \right]. \tag{2.23}$$

In this expression, the coefficients A_n ($n = 0, 1, 2$) are independent of λ and remain to be determined. The functions $W_\pm(\lambda)$ are, respectively, regular and non-zero in $\mathrm{Im}(\lambda) \gtrless 0$, satisfy $W(\lambda) = W_+(\lambda)W_-(\lambda)$, $W_\pm(\pm\lambda) = W_\mp(\mp\lambda)$ and $|W_\pm(\lambda)| \sim O(|\lambda|^{7/2})$ as $|\lambda| \to \infty$ (Howe 1993*c*). They are conveniently represented in their respective domains of regularity by the formula

$$W_\pm(\lambda) = e^{i\pi/4}(i\pm\lambda)^{3/2}(K_\eta \pm \lambda)(K_s \pm \lambda) \exp\left(\pm \frac{1}{2\pi i} \int_{-\infty}^{\infty} \frac{\ln\{Z(\xi)\}}{\xi-\lambda}\, d\xi \right), \quad \mathrm{Im}\,\lambda \gtrless 0, \tag{2.24}$$

where

$$Z(\lambda) = \frac{W(\lambda)}{(K_\eta^2-\lambda^2)(K_s^2-\lambda^2)(1+\lambda^2)^{3/2}}. \tag{2.25}$$

The function $Z(\lambda)$ is finite and non-zero on the real axis, and $Z(\lambda) \to +1$ as $\lambda \to \pm\infty$.

Equation (2.10) for the radial displacement ζ now becomes

$$\frac{\zeta}{\zeta_I+\zeta_0} = e^{i\Lambda X} - \frac{P(\Lambda)W_+(\Lambda)}{2\pi i \sigma_2(\Lambda^2-\alpha^2\mu^2)} \int_{-\infty}^{\infty} \frac{f(\lambda)\sqrt{\lambda^2-\mu^2}}{W_+(\lambda)} \times \left[\frac{1}{\lambda-\Lambda-i0} + A_0 + A_1\lambda + A_2\lambda^2 \right] e^{i\lambda X}\, d\lambda, \quad X<0, \tag{2.26}$$

and the values of the coefficients A_0, A_1, A_2 are determined by application of the boundary conditions (2.15). To do this we first note that, since $[p_s] \to 0$ as $X \to -0$, the second of equations (2.5) permits the edge conditions to be written

$$\frac{\partial^2\zeta}{\partial X^2} = 0, \quad \frac{\partial^3\zeta}{\partial X^3} = 0, \quad \left(\frac{\partial^4}{\partial X^4} - 1 + \frac{(1-\sigma^2)}{(\alpha\mu A)^2} \right) \zeta = 0, \quad X \to -0. \tag{2.27}$$

Using (2.26), these conditions are found to supply the following equations for A_0, A_1, A_2:

$$\sum_{j=0}^{2} C_{ij} A_j = B_i, \quad i = 0, 1, 2, \tag{2.28}$$

where

$$\left.\begin{aligned} &C_{00}=S_2^+,\quad C_{01}=C_{10}=S_3^-,\quad C_{02}=C_{11}=S_4^+,\quad C_{12}=S_5^-,\\ &C_{20}=S_4^+-\left(1-\frac{(1-\sigma^2)}{(\alpha\mu A)^2}\right)S_0^+,\quad C_{21}=S_5^--\left(1-\frac{(1-\sigma^2)}{(\alpha\mu A)^2}\right)S_1^-,\\ &C_{22}=S_6^+-\left(1-\frac{(1-\sigma^2)}{(\alpha\mu A)^2}\right)S_2^+,\\ &B_0=T_2^-,\quad B_1=T_3^+,B_2=T_4^--\left(1-\frac{(1-\sigma^2)}{(\alpha\mu A)^2}\right)T_0^-, \end{aligned}\right\} \tag{2.29}$$

$$\left.\begin{aligned} &S_n^\pm=\textstyle\sum_j\lambda_j^nF_\pm(\lambda_j),\quad T_n^\pm=\sum_j\frac{\lambda_j^n[\lambda_jF_\pm(\lambda_j)+\Lambda F_\mp(\lambda_j)]}{\Lambda^2-\lambda_j^2},\\ &F_\pm(\lambda)=\frac{\sigma_2(\lambda^2-\alpha^2\mu^2)\pm\{W_+(\lambda)\}^2}{W_+(\lambda)P'(\lambda)}. \end{aligned}\right\} \tag{2.30}$$

In (2.30), $P'(\lambda)=\partial P(\lambda)/\partial\lambda$, and the summation is taken over the three zeros λ_1, λ_2, λ_3 of $P(\lambda)$ that are either real and positive or have positive imaginary part.

(*e*) *Green's function*

An expression for the total pressure p in terms of expression (2.23) for $\mathcal{I}(\lambda)\equiv\bar{\mathcal{I}}(\lambda K_0)$ may now be written down by substituting into (2.11). The final result is simplified by indenting the integration contour along the real k-axis to pass *above* the pole of $\mathcal{I}(\lambda)$ at $\lambda\equiv k/K_0=\lambda+\mathrm{i}0$. In each of (2.11 *a*), (2.11 *b*), the residue contribution captured in this way cancels the second term on the right-hand side, and the two expressions for the pressure may then be combined in the form

$$\begin{aligned}\frac{p}{\rho_0c_0^2}=\frac{p_{\mathrm{I}}}{\rho_0c_0^2}&-\frac{\zeta_0\mu^2W_+(\Lambda)}{2\pi f(\Lambda)\sqrt{\Lambda^2-\mu^2}}\int_{-\infty}^{\infty}\frac{f(\lambda)}{W_+(\lambda)}\left[\frac{1}{\lambda-\Lambda+\mathrm{i}0}+\sum_{n=0}^{2}A_n\lambda^n\right]\\ &\times\left(\frac{H_0^{(1)}\{\gamma(k)r\}}{H_1^{(1)}\{\gamma(k)a\}}H(r-a)+\frac{J_0\{\gamma(k)r\}}{J_1\{\gamma(k)a\}}H(a-r)\right)\mathrm{e}^{\mathrm{i}kx}\,\mathrm{d}k,\end{aligned} \tag{2.31}$$

where $\lambda=k/K_0$, and the notation $1/(\lambda-\Lambda+\mathrm{i}0)$ is a reminder that the pole is now below the integration contour.

The second term on the right-hand side of (2.31) is equal to p_{s}/ρ_0c_2. Inserting this expression for p_{s} into equation (2.4), and making use of the definition (2.12) of ζ_0, we finally obtain the following representation of the axisymmetric Green's function:

$$\begin{aligned}G_{\mathrm{p}}(x,\bar{x},r,\bar{r},t-\tau)&=G'_{\mathrm{p}}(x,\bar{x},r,\bar{r},t-\tau)\\ &+\frac{1}{32\pi^3}\int_{-\infty}^{\infty}\frac{f(\lambda)\sqrt{\Lambda^2-\mu^2}P(\Lambda)H_1^{(1)}\{\gamma(\kappa)a\}J_0\{\gamma(\kappa)\bar{r}\}}{K_0W_-(\Lambda)W_+(\lambda)}\\ &\times\left[\frac{1}{\lambda-\Lambda+\mathrm{i}0}+\sum_{n=0}^{2}A_n\lambda^n\right]\left(\frac{H_0^{(1)}\{\gamma(k)r\}}{H_1^{(1)}\{\gamma(k)a\}}H(r-a)+\frac{J_0\{\gamma(k)r\}}{J_1\{\gamma(k)a\}}H(a-r)\right)\\ &\times\mathrm{e}^{\mathrm{i}\{kx-\kappa\bar{x}-\omega(t-\tau)\}}\,\mathrm{d}k\,\mathrm{d}\kappa\,\mathrm{d}\omega,\quad \bar{r}<a,\end{aligned} \tag{2.32}$$

where $\Lambda=\kappa/K_0$.

This formula is applicable for a ring source of radius $\bar{r} < a$. For arbitrary source position we find

$$G_{\rm p}(x,\bar{x},r,\bar{r},t-\tau) = G'_{\rm p}(x,\bar{x},r,\bar{r},t-\tau)$$
$$-\frac{1}{32\pi^4}\int_{-\infty}^{\infty}\frac{f(\lambda)f(\Lambda)P(\Lambda)}{K_0^2 aW_-(\Lambda)W_+(\lambda)}\left[\frac{1}{\lambda-\Lambda+{\rm i}0}+\sum_{n=0}^{2}A_n\lambda^n\right]$$
$$\times\left(\frac{H_0^{(1)}\{\gamma(\kappa)\bar{r}\}}{H_1^{(1)}\{\gamma(\kappa)a\}}H(\bar{r}-a)+\frac{J_0\{\gamma(\kappa)\bar{r}\}}{J_1\{\gamma(\kappa)a\}}H(a-\bar{r})\right)$$
$$\times\left(\frac{H_0^{(1)}\{\gamma(k)r\}}{H_1^{(1)}\{\gamma(k)a\}}H(r-a)+\frac{J_0\{\gamma(k)r\}}{J_1\{\gamma(k)a\}}H(a-r)\right)$$
$$\times{\rm e}^{{\rm i}\{kx-\kappa\bar{x}-\omega(t-\tau)\}}\,{\rm d}k\,{\rm d}\kappa\,{\rm d}\omega. \tag{2.33}$$

3. Approximations for compact source distributions

In analysing aerodynamic sound problems, it is frequently permissible to assume that the length scale of the source (the turbulence correlation scale, for example) is small ('compact') compared to the characteristic structural wavelength. In the representation (2.33) of Green's function, $1/\Lambda \equiv K_0/\kappa$ may be taken as a non-dimensional measure of the source length scale. The corresponding scale of the smallest structural motions is of order $1/|\lambda_j|_{\max}$, where $|\lambda_j|_{\max} \equiv$ the maximum modulus of the zeros of $P(\lambda)$. Thus, the source is compact with respect to the structural vibrations provided the dominant values of Λ arising in the noise generation problem satisfy

$$|\Lambda| \gg |\lambda_j|_{\max} \tag{3.1}$$

The integrand of (2.33) can then be simplified by expanding in powers of $|\lambda_j|_{\max}/\Lambda$. The resulting expression for Green's function is applicable when the characteristic dimension of a turbulent eddy is small compared to the wavelengths of the structural waves that it generates, and the mechanics of the local flow are then essentially the same as for a *rigid* walled duct.

We first examine the behaviour of the coefficients A_n when Λ is large, and then consider various additional approximations that are valid at low frequencies.

(*a*) *Asymptotic expansion of* A_n

In equations (2.28) for A_0, A_1, A_2, only the coefficients B_0, B_1, B_2 depend on Λ. Reference to the definition (2.30) of $T_n^{\pm}$ indicates that B_0, B_1, B_2 can be expanded in a convergent power series in $1/\Lambda$ provided condition (3.1) is satisfied. It is then easy to see that A_i possesses an asymptotic expansion of the form

$$A_i = \frac{1}{\Lambda^{i+1}} + \frac{1}{\Lambda^4}\sum_{n=0}^{\infty}\frac{a_{in}}{\Lambda^n}, \quad |\Lambda| \gg |\lambda_j|_{\max}, \quad i = 0,1,2. \tag{3.2}$$

For each fixed value of n, the coefficients a_{in} satisfy

$$\sum_{j=0}^{2} C_{ij}a_{jn} = b_{in}, \quad i = 0,1,2, \tag{3.3}$$

where the C_{ij} are defined as in (2.29),

$$\left.\begin{aligned} b_{0n} &= \textstyle\sum_j \lambda_j^{5+n} F_{(-)^{n+1}}(\lambda_j), \quad b_{1n} = \sum_j \lambda_j^{6+n} F_{(-)^n}(\lambda_j), \\ b_{2n} &= \left[\lambda_j^4 - \left(1 - \frac{(1-\sigma^2)}{(\alpha\mu A)^2}\right)\right] \lambda_j^{3+n} F_{(-)^{n+1}}(\lambda_j), \end{aligned}\right\} \tag{3.4}$$

and the summations in (3.4) are taken over the three roots λ_1, λ_2, λ_3 of $P(\lambda)$, as before.

The term in square brackets in the integrand (2.33) has the corresponding expansion:

$$\frac{1}{\lambda - \Lambda + \mathrm{i}0} + A_0 + A_1\lambda + A_2\lambda^2 = \frac{1}{\Lambda^4} \sum_{n=0}^{\infty} \frac{a_{0n} + a_{1n}\lambda + a_{2n}\lambda^2 - \lambda^3}{\Lambda^n}, \quad \Lambda > \lambda. \tag{3.5}$$

(*b*) *Behaviour of a_{in} at low frequencies*

The effect of fluid loading is especially important at low frequencies, and it will be shown that the response of the duct to forcing by the source flow completely dominates the radiation characteristics when $\omega < \omega_{\mathrm{R}} \equiv c/a$ (the ring frequency). At such low frequencies the limiting form of the dimensionless dispersion function $W(\lambda)$ (see equation (2.20)) suggests that the non-dimensional groupings governing the coefficients a_{in} are $(\omega/\omega_{\mathrm{R}})/\sqrt{1-\sigma^2}$ and a/h. If we write

$$a_{in} = c_{in} \left(\frac{\omega/\omega_{\mathrm{r}}}{\sqrt{1-\sigma^2}}\right)^{n_\omega} \left(\frac{a}{h}\right)^{n_a}, \quad wa/c \ll 1, \tag{3.6}$$

it might then be expected that the values of the constants c_{in} and the exponents n_ω, n_a can be obtained from the numerical solution of the equations (3.3) by logarithmic differencing. The results of such a calculation are given in table 1 for $n = 0$, 1 and 2. A detailed examination of the numerical data indicates that the starred entries in the table are *not* constants, but exhibit a more complicated dependence on the physical parameters than is accounted for by the hypothesis (3.6). However, the variations are small (typical departures from the tabulated values being of order 1%), and table 1 may be taken to define the principal properties of scattering at low frequencies. More accurate values of c_{00}, c_{01}, c_{02} and c_{22} for a steel duct in water at different values of a/h are given in table 2.

It may be surmised from table 1 that

$$\frac{a_{0(n+1)}}{a_{0n}} \sim \frac{a_{1,(n+1)}}{a_{1,n}} \approx \frac{1}{\sqrt{\omega/\omega_{\mathrm{r}}}} \equiv \frac{1}{\sqrt{\alpha\mu A}}. \tag{3.7}$$

For these coefficients, successive terms in expansion (3.2) decrease by a factor $\sim 1/\{\Lambda\sqrt{\omega/\omega_{\mathrm{R}}}\}$. This is small when (3.1) is satisfied, since, when the frequency ω is smaller than the ring frequency c/a, definition (2.20) of $P(\lambda)$ implies that $|\lambda_j|_{\max} \sim 1/\sqrt{\omega/\omega_{\mathrm{r}}}$.

(*c*) *Compact approximation for aerodynamic sources near the nozzle exit*

In low Mach number flows, the turbulence aerodynamic sound sources are generally also *acoustically* compact, i.e. the wavelength of the generated sound is much larger than the typical eddy scale. This indicates that the most important contributions to (2.33) are from values of Λ satisfying $\Lambda \gg \mu$. Furthermore, except at extremely

Table 1. *Parameters defining the asymptotic formula (3.6)*

	c_{in}	n_ω	n_a
a_{00}	0.537^{a}	$-\frac{1}{2}$	$-\frac{1}{2}^{\mathrm{a}}$
a_{10}	1	-1	0
a_{20}	$-\mathrm{i}\sqrt{2}$	$-\frac{1}{2}$	0
a_{01}	$-\mathrm{i}0.760^{\mathrm{a}}$	-1	$-\frac{1}{2}^{\mathrm{a}}$
a_{11}	$-\mathrm{i}\sqrt{2}$	$-\frac{3}{2}$	0
a_{21}	-1	-1	0
a_{02}	-0.537^{a}	$-\frac{3}{2}$	$-\frac{1}{2}^{\mathrm{a}}$
a_{12}	-1	-2	0
a_{22}	0.537^{a}	$-\frac{1}{2}$	$-\frac{1}{2}^{\mathrm{a}}$

[a]Approximate value.

low frequencies, the turbulence scale will usually be much smaller than the radius a of the duct (even for fully developed pipe flow, the eddy scale is typically less than $0.2a$ (Hinze 1975)). This means that $\kappa a \equiv \Lambda A \gg 1$, and that only turbulence eddies within a turbulence correlation scale ($\sim 1/\Lambda$) of the nozzle lip will interact significantly with the nozzle. This can be used to simplify (2.32) and (2.33).

Using the definitions (2.24), (2.25), and the asymptotic formulae for Bessel and Hankel functions (Abramowitz & Stegun 1970), we can write

$$\frac{\sqrt{\Lambda^2-\mu^2}P(\Lambda)H_1^{(1)}\{\gamma(\kappa)a\}J_0\{\gamma(\kappa)\bar{r}\}}{W_-(\Lambda)} \approx \frac{-\Lambda^{5/2}\mathrm{e}^{-\{|\kappa|(a-\bar{r})-\pi\mathrm{i}/4\}}}{\pi K_0 a}, \quad \text{for } |\Lambda| \gg \mu,\ |\lambda|_{\max},\ 1/A, \tag{3.8}$$

where $\Lambda^{1/2} = -\mathrm{i}|\Lambda|^{1/2}$ for $\Lambda < 0$. Inserting this into the integrand of (2.32) (for $a > \bar{r}$) and taking the leading-order term in the expansion (3.5), we then find

$$\begin{aligned} G_{\mathrm{p}}(x,\bar{x},r,\bar{r},t-\tau) \approx\ & G'_{\mathrm{p}}(x,\bar{x},r,\bar{r},t-\tau) \\ & -\frac{\mathrm{e}^{\mathrm{i}\pi/4}}{2(2\pi)^4 a}\int_{-\infty}^{\infty}\frac{\mathrm{e}^{-|\kappa|(a-\bar{r})}}{\sqrt{K_0}(\kappa-\mathrm{i}0)^{3/2}} \\ & \times\frac{f(\lambda)}{W_+(\lambda)}(a_{00}+a_{10}\lambda+a_{20}\lambda^2-\lambda^3) \\ & \times\left(\frac{H_0^{(1)}\{\gamma(k)r\}}{H_1^{(1)}\{\gamma(k)a\}}H(r-a)+\frac{J_0\{\gamma(k)r\}}{J_1\{\gamma(k)a\}}H(a-r)\right) \\ & \times\mathrm{e}^{\mathrm{i}\{kx-\kappa\bar{x}-\omega(t-\tau)\}}\,\mathrm{d}\kappa\,\mathrm{d}k\,\mathrm{d}\omega. \end{aligned} \tag{3.9}$$

In this approximation, it is necessary to interpret the integral with respect to κ as a generalized function (Lighthill 1958; Jones 1982), yielding

$$\int_{-\infty}^{\infty}\frac{\mathrm{e}^{-|\kappa|(a-\bar{r})-\mathrm{i}\kappa\bar{x}}}{(\kappa-\mathrm{i}0)^{3/2}}\,\mathrm{d}\kappa = 4\sqrt{\pi}\mathrm{e}^{-\mathrm{i}\pi/4}\sqrt{R}\sin(\Theta/2)+\text{const.}, \tag{3.10}$$

where (R, Θ) are polar coordinates of the ring source relative to the lip (see figure 2), i.e.

$$R = \{(a-\bar{r})^2 + \bar{x}^2\}^{1/2}, \quad \Theta = \arcsin\left(\frac{\bar{r}-a}{R}\right). \tag{3.11}$$

The constant in (3.10) can be discarded since aerodynamic sources are either dipoles or quadrupoles, and expressions for the aerodynamic sound will therefore involve one or more of the derivatives $\partial G_{\rm p}/\partial R$, $\partial G_{\rm p}/\partial \Theta$, and the contribution from the constant is then null. Hence, we can take

$$\begin{aligned} G_{\rm p}(x,\bar{x},r,\bar{r},t-\tau) \approx G'_{\rm p}(x,\bar{x},r,\bar{r},t-\tau) \\ -\frac{\sqrt{R}\sin(\Theta/2)}{\sqrt{\pi}(2\pi)^3 a}\int_{-\infty}^{\infty}\frac{f(\lambda)}{\sqrt{K_0}W_+(\lambda)}(a_{00}+a_{10}\lambda+a_{20}\lambda^2-\lambda^3) \\ \times\left(\frac{H_0^{(1)}\{\gamma(k)r\}}{H_1^{(1)}\{\gamma(k)a\}}H(r-a)+\frac{J_0\{\gamma(k)r\}}{J_1\{\gamma(k)a\}}H(a-r)\right) \\ \times \mathrm{e}^{\mathrm{i}\{kx-\omega(t-\tau)\}}\,\mathrm{d}k\,\mathrm{d}\omega. \end{aligned} \tag{3.12}$$

This formula has been derived for source radius $\bar{r} < a$, but the same result is obtained when $\bar{r} > a$.

(*d*) *The acoustic far field*

The pressure at large distances from the nozzle exit is determined, for each frequency ω, by the asymptotic value as $\kappa_0|\boldsymbol{x}| \to \infty$ of the integration in (3.12) with respect to k, where $|\boldsymbol{x}| \equiv \sqrt{r^2+x^2}$. This may be evaluated by the method of steepest descents (Watson 1944). To a first approximation, this is equivalent to the method of stationary phase: as $r \to \infty$, the Hankel function $H_0^{(1)}\{\gamma(k)r\}$ is replaced by its large argument approximation $H_0^{(1)}(z) \approx (2/\pi z)^{1/2}\mathrm{e}^{\mathrm{i}(z-\pi/4)}$, $|z| \to \infty$ (Abramowitz & Stegun 1970). The integrand then contains the rapidly fluctuating factor $\mathrm{e}^{\mathrm{i}\{kx+\gamma(k)r\}}$, which is expanded to second order in powers of k about $k = \kappa_0\cos\theta$, where θ is the radiation direction defined by $x = |\boldsymbol{x}|\cos\theta$, $r = |\boldsymbol{x}|\sin\theta$ (see figure 2), and $k = \kappa_0\cos\theta$ is the wavenumber whose component of phase velocity ω/k in the θ-direction is precisely equal to the speed of sound c_0. The integral can then be evaluated analytically after first setting $k = \kappa_0\cos\theta$ elsewhere in the integrand. This yields,

$$\begin{aligned} G_{\rm p}(x,\bar{x},r,\bar{r},t-\tau) \approx G'_{\rm p}(x,\bar{x},r,\bar{r},t-\tau) \\ +\frac{\mathrm{i}\sqrt{R}\sin(\Theta/2)\sin\theta}{4\pi^{5/2}|\boldsymbol{x}|}\int_{-\infty}^{\infty}\frac{\mu\sqrt{K_0}J_1(\kappa_0 a\sin\theta)}{W_+(\mu\cos\theta)} \\ \times(a_{00}+a_{10}\mu\cos\theta+a_{20}\mu^2\cos^2\theta-\mu^3\cos^3\theta) \\ \times\mathrm{e}^{\mathrm{i}\omega\{t-\tau-|\boldsymbol{x}|/c_0\}}\,\mathrm{d}\omega, \quad |\boldsymbol{x}| \to \infty. \end{aligned} \tag{3.13}$$

This approximation is uniformly valid in θ provided the integrand of (3.12) has no poles near the real k-axis in the *acoustic domain* $|k| < |\kappa_0|$. According to (2.24), however, and the discussion of § 2 (*b*), there is a pole at $k = -\kappa_\eta$ ($\lambda = -K_\eta$), which approaches the acoustic interval of the real axis near $k = -\omega/c \equiv -\alpha\kappa_0$, when ω is smaller than the ring frequency c/a. It corresponds to a structural disturbance excited at the nozzle exit which propagates towards $x = -\infty$ with phase velocity $\approx c > c_0$. This is a *leaky wave*, whose amplitude decreases slowly with propagation distance $-x$ as its energy is radiated into the fluid as sound.

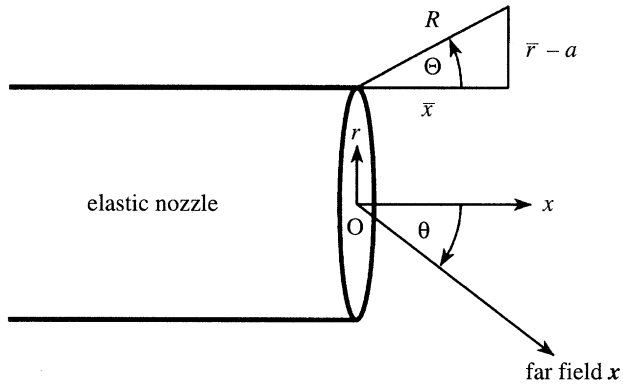

Figure 2. The near field and far field coordinates (R, Θ) and $(|\boldsymbol{x}|, \theta)$.

The leaky wave decays over an axial distance along the duct $\sim O(1/\epsilon\kappa_0)$, where ϵ is the fluid loading parameter. Therefore, the approximation (3.13) becomes uniform when $|\boldsymbol{x}|$ lies beyond the Fresnel diffraction zone of this length, i.e. for $|\boldsymbol{x}| > O\{1/(\epsilon^2\kappa_0)\}$ (Born & Wolf 1975). If the pressure is required in the Fresnel region, a more careful application of the method of steepest descents must be made, involving a deformation of the integration contour in (3.12) into the complex k-plane and the capture of a residue contribution from the pole when the radiation angle θ exceeds the leaky wave angle $\arccos(-c_0/c)$ (Jones 1964; Landau & Lifshitz 1987). However, the approximation (3.13) is perfectly adequate for calculating the net radiated sound power, and is sufficient for the present discussion.

(*e*) *Green's function for a rigid nozzle*

At very high frequencies ($\omega/\omega_c \gg 1$), the influence of fluid loading of the nozzle is small, and the radiation field is the same as that produced by a ring source in the vicinity of a *rigid* nozzle exit. In this limit, all length scales in the fluid are small relative to the structural wavelengths. Green's function for this case has been analysed by Leppington (1971); the particular form corresponding to the far field expression (3.13) for the elastic duct is obtained from (3.13) by letting $\mu \to \infty$.

In this limit, $K_s \to \mu - 0$, and definition (2.24) can be used to deduce that

$$\left.\begin{aligned} W_+(\lambda) &\approx \mathrm{e}^{\mathrm{i}\pi/4}\sqrt{A}\lambda^3(\lambda+\mu)\bar{W}_+(\lambda), \quad \lambda \approx 0(\mu) \gg 1, \\ \bar{W}_+(\lambda) &= \exp\left(\frac{\lambda}{\pi\mathrm{i}}\int_0^\infty \frac{\ln[\pi H_1^{(1)}(A\sqrt{\mu^2-\xi^2})J_1(\sqrt{\mu^2-\xi^2})]\,\mathrm{d}\xi}{\xi^2-\lambda^2}\right), \quad \mathrm{Im}\{\lambda\} > 0. \end{aligned}\right\} \tag{3.14}$$

Hence, retaining only the final term in μ^3 in the brace brackets of the integrand (3.13), the far field form of the axisymmetric Green's function for the rigid duct is found to be

$$G_p(x,\bar{x},r,\bar{r},t-\tau) \approx G_p'(x,\bar{x},r,\bar{r},t-\tau) - \frac{\mathrm{e}^{\mathrm{i}\pi/4}\sqrt{R}\sin(\Theta/2)\{1-\cos\theta\}}{4\pi^{5/2}|\boldsymbol{x}|\sqrt{a}\sin\theta} \times \int_{-\infty}^{\infty} \frac{J_1(\kappa_0 a\sin\theta)}{\bar{W}_+(\mu\cos\theta)}\mathrm{e}^{-\mathrm{i}\omega\{t-\tau-|\boldsymbol{x}|/c_0\}}\,\mathrm{d}\omega, \quad |\boldsymbol{x}| \to \infty. \tag{3.15}$$

When $A = K_0 a$ is large, $J_1(A\sqrt{\mu^2-\xi^2})$ has many zeros on the real axis in $0 < \xi < \mu$,

and the definition (3.14) implies that many of these are shared by $\bar{W}_+(\lambda)$. They correspond to acoustic modes of the hard walled duct.

When the nozzle is acoustically compact, $\kappa_0 a \equiv \omega a/c_0 \ll 1$ for all relevant frequencies. In this limit, it is easily deduced from (3.14) that $\bar{W}_+(\mu\cos\theta) \to \mathrm{e}^{\mathrm{i}\pi/4}$, and (3.15) then reduces to

$$G_\mathrm{p}(x,\bar{x},r,\bar{r},t-\tau) \approx G'_\mathrm{p}(x,\bar{x},r,\bar{r},t-\tau) + \frac{\sqrt{aR}\sin(\Theta/2)\{1-\cos\theta\}}{4\pi^{3/2}c_0|\boldsymbol{x}|}\delta'\{t-\tau-|\boldsymbol{x}|/c_0\}, \tag{3.16}$$

where the prime denotes differentiation with respect to time. This formula agrees with the result given by Leppington (1971).

4. Acoustic and structural power radiated by a time harmonic source

(*a*) *The scattered acoustic and flexural waves*

We now examine the sound and structural vibrations produced by a time harmonic ring source (x_0, r_0) close to the lip of the nozzle, such that the pressure p is governed by the equation

$$\left(\frac{1}{c_0^2}\frac{\partial^2}{\partial t^2} - \nabla^2\right) p = \mathcal{L}\left(\frac{1}{2\pi r}\delta(x-x_0)\delta(r-r_0)\mathrm{e}^{-\mathrm{i}\omega t}\right), \quad \omega > 0 \tag{4.1}$$

where the real part of the term on the right-hand side is to be taken, and $\mathcal{L}$ is a differential operator determined by the multipole order of the source.

The solution of this equation with outgoing wave behaviour is given by

$$p(\boldsymbol{x},t) = \frac{1}{r_0}\int G_\mathrm{p}(x,\bar{x},r,\bar{r},t-\tau)\bar{\mathcal{L}}(\delta(\bar{x}-x_0)\delta(\bar{r}-r_0)\mathrm{e}^{-\mathrm{i}\omega\tau})\bar{r}\,\mathrm{d}\bar{r}\,\mathrm{d}\bar{x}\,\mathrm{d}\tau, \tag{4.2}$$

where the integrations are over the whole of the fluid and all times τ, and the notation $\bar{\mathcal{L}}$ implies that the operator $\mathcal{L}$ acts on the variables $\bar{r}$, $\bar{x}$. Integrating by parts, we find

$$p(\boldsymbol{x},t) = \frac{\mathrm{e}^{-\mathrm{i}\omega t}}{r_0}\int_{-\infty}^{\infty}\mathcal{L}'_0\{r_0 G_\mathrm{p}(x,x_0,r,r_0,\tau)\}\mathrm{e}^{\mathrm{i}\omega\tau}\,\mathrm{d}\tau, \tag{4.3}$$

where $\mathcal{L}'_0$ is the adjoint of $\mathcal{L}$ and acts on the source variables r_0, x_0.

In the acoustic far field, the component of the pressure due to the interaction of the source with the nozzle is obtained by replacing G_p by the second term on the right-hand side of (3.13). The result can be written

$$p(\boldsymbol{x},t) \approx \frac{-\mathrm{i}p_0\ell^{3/2}}{|\boldsymbol{x}|}\frac{\mu\sqrt{K_0}\sin\theta J_1(\kappa_0 a\sin\theta)}{W_+(\mu\cos\theta)} \times(a_{00}+a_{10}\mu\cos\theta+a_{20}\mu^2\cos^2\theta-\mu^3\cos^3\theta)\mathrm{e}^{-\mathrm{i}\omega(t-|\boldsymbol{x}|/c_0)}, \quad |\boldsymbol{x}|\to\infty, \tag{4.4}$$

where it is convenient to introduce characteristic source pressure and length scales p_0 and ℓ, respectively, which are defined to satisfy

$$p_0\ell^{3/2} \equiv \frac{1}{2\pi^{3/2}r_0}\mathcal{L}'_0\{r_0\sqrt{R_0}\sin(\Theta_0/2)\}, \quad R_0 \ll 1, \tag{4.5}$$

where R_0, Θ_0 are the polar coordinates of the source relative to the nozzle lip (cf. figure 2).

To calculate the flexural response of the duct it is necessary to use the more general formula (3.12) for $G_{\rm p}$, in terms of which, and for $r > a$, the scattered pressure is given by

$$p(\boldsymbol{x},t) \approx \frac{-p_0\ell^{3/2}}{2\pi a}\int_{-\infty}^{\infty}\frac{f(\lambda)H_0^{(1)}\{\gamma(k)r\}}{\sqrt{K_0}W_+(\lambda)H_1^{(1)}\{\gamma(k)a\}} \times(a_{00}+a_{10}\lambda+a_{20}\lambda^2-\lambda^3)\mathrm{e}^{\mathrm{i}(kx-\omega t)}\,\mathrm{d}k, \quad r>a. \tag{4.6}$$

The radial displacement of the duct wall caused by scattering is now obtained by substituting this expression for p into equation (2.9):

$$\zeta(x,t) = \frac{p_0\ell^{3/2}}{2\pi a\rho_0\omega^2\sqrt{K_0}}\int_{-\infty}^{\infty}\frac{\gamma(k)f(\lambda)}{W_+(\lambda)}(a_{00}+a_{10}\lambda+a_{20}\lambda^2-\lambda^3)\mathrm{e}^{\mathrm{i}(kx-\omega t)}\,\mathrm{d}k. \tag{4.7}$$

(*b*) *Radiated sound power*

The sound power $\Pi_{\rm A}$, say, is calculated by integrating the *acoustic intensity* $\langle p^2\rangle/\rho_0 c_0$ over the surface of a large sphere of radius $|\boldsymbol{x}|$. The angle brackets denote a time average, which is evaluated from (4.4) after taking the real part. The result can be written

$$\frac{\rho_0 c_0 \Pi_{\rm A}}{|p_0|^2\ell^2} = 2\pi|\boldsymbol{x}|^2\int_0^{\pi}\frac{\langle p^2\rangle\sin\theta}{|p_0|^2\ell^2}\,\mathrm{d}\theta = 2\Pi\int_0^{\pi}\Phi(\omega,\theta)\sin\theta\,\mathrm{d}\theta, \tag{4.8a}$$

$$\Phi \equiv \frac{\ell\mu^2 K_0\sin^2\theta\{J_1(\kappa_0 a\sin\theta)\}^2}{2|W_+(\mu\cos\theta)|^2}|a_{00}+a_{10}\mu\cos\theta+a_{20}\mu^2\cos^2\theta-\mu^3\cos^3\theta|^2. \tag{4.8b}$$

In these equations $\Phi(\omega,\theta)$ is the directivity of the sound, which is equal to the sound power radiated per unit solid angle in direction θ. Although the method of stationary phase has been used to derive expression (4.4) for p used in (4.8), this is not really necessary, since (4.8) can also be obtained directly from the general representation (4.6) of the pressure in $r > a$ by considering the energy flux through the cylinder $r = a$ and isolating that part associated with the sound (as opposed to the fluid-coupled flexural vibrations).

The directivity $\Phi(\omega,\theta)$ is plotted in figure 3*a* for different values of $\omega/\omega_{\rm c}$ (not to the same scales) for a steel duct in water ($\epsilon \approx 0.135$; $\alpha = 0.275$) and the typical value $a/h = 100$. In obtaining these figures the values of the coefficients a_{00}, a_{10}, a_{20} in (4.8) are determined from the numerical solution of equations (3.3). When $\omega/\omega_{\rm c} = 0.1$ ($\kappa_0 a \approx 9.5$), the acoustic wavelength is about three times the duct diameter, and the directivity exhibits a characteristic multilobed structure. At the ring frequency $\omega/\omega_{\rm c} = (h/a)/\{\alpha^2\sqrt{12}\} \approx 0.038$, the field shape has two broad lobes and a very sharp spike in the leaky wave direction $\theta = \theta_{\rm L} \approx \arccos(-\alpha) \approx 106°$. The spike is caused by the approach of the zero $\lambda = -K_\eta$ of $W_+(\lambda)$ to the real axis at $\mu\cos\theta = -\operatorname{Re} K_\eta \approx -\alpha\mu$. At $\omega/\omega_{\rm c} = 0.02$, the directivity has a single lobe peaking at $\theta = 90°$ together with a leaky wave spike. The striking appearance of this spike arises because the last factor on the right of (4.8*b*) (involving the a_{i0}) is small in the neighbourhood of the leaky wave angle, and this nullifies the influence of the leaky wave pole except in the immediate vicinity of $\theta_{\rm L}$. This is also evident in the final example of figure 3*a* ($\omega/\omega_{\rm c} = 0.001$), although the leaky wave contribution is now very much larger. A further reduction in frequency does not change the character of the field shape, but the power in the lobe ultimately becomes insignificant compared

PHILOSOPHICAL TRANSACTIONS OF THE ROYAL SOCIETY A MATHEMATICAL, PHYSICAL & ENGINEERING SCIENCES

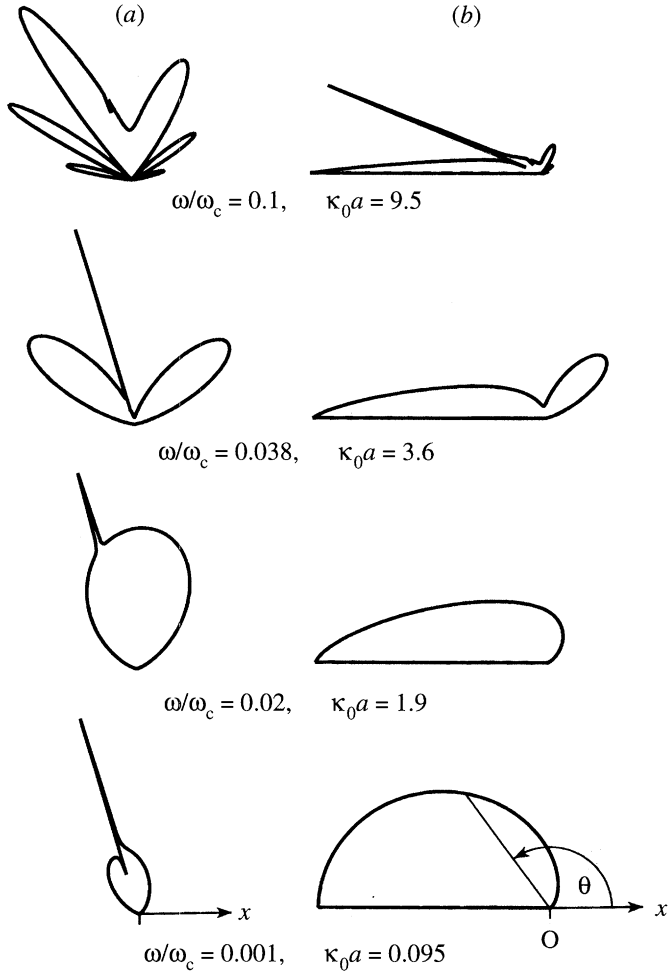

Figure 3. Directivity of the scattered sound: (*a*) steel nozzle in water with $a/h = 100$; (*b*) rigid nozzle.

to the leaky wave power. In this limit, Φ is *independent of frequency* (see § 4 *d*), and all of the acoustic radiation is launched by the leaky mode. For comparison, figure 3*b* depicts the corresponding fields shapes for a rigid nozzle, calculated by use of the Green's function (3.15).

That the final factor on the right-hand side of (4.8 *b*) is small near $\theta = \theta_{\mathrm{L}}$ can be deduced by consideration of the third ($i = 2$) of equations (3.3) for the coefficients a_{i0}. It follows from (2.29), (2.30) and (3.4) that each of the coefficients C_{20}, C_{21}, C_{22}, b_{20} in that equation consists of a summation involving the zeros λ_j of $P(\lambda)$, each term of which contains the factor

$$\left[\lambda_j^4 - \left(1 - \frac{(1-\sigma^2)}{(\alpha\mu A)^2}\right)\right].$$

This is small ($\sim \pm \mathrm{i}\alpha^2(h/a)/\sqrt{12(1-\sigma^2)}$) when $\alpha\mu A \equiv \omega a/c \to 0$ for two of the zeros, λ_2, λ_3, say, but large ($\sim (1-\sigma^2)/(\alpha\mu A)^2$) for the third root $\lambda_1 \approx \alpha\mu$. Since also $F_+(\alpha\mu) = -F_-(\alpha\mu)$, it can be seen that, in the leading approximation, the third

of equations (3.3) reduces to

$$a_{00} - \alpha\mu a_{10} + (\alpha\mu)^2 a_{20} + (\alpha\mu)^3 \approx 0,$$

which proves our contention, since $\cos\theta_{\rm L} \approx -\alpha$.

(c) *The leaky wave power*

To clarify the role of the leaky wave, it is useful to calculate explicitly the sound power $\Pi_{\rm L}$ radiated by this wave. This can be done by confining the integration angle in (4.8) to a small interval enclosing the leaky wave direction $\theta_{\rm L}$, or by making use of the following generalization (proved in the appendix) of the formula for the power transmitted by an evanescent surface wave (Howe 1992):

$$\Pi_{\rm L} = \tfrac{1}{2}\pi a\omega|\zeta_\eta|^2 \left|\frac{\partial D}{\partial k}(k,\omega)\right|_{k=-\kappa_\eta}, \tag{4.9}$$

where ζ_η is the complex amplitude at $x = 0$ of the leaky wave, and D is the dispersion function defined as in (2.13). In the acoustic domain, D is complex and the modulus of its derivative is to be taken.

The value of ζ_η is given by the residue contribution to the integral (4.7) from the pole at $\lambda = -K_\eta$, where $W_+(\lambda) \equiv W(\lambda)/W_-(\lambda) = 0$; the pole is just below the real λ-axis in the vicinity of the acoustic interval $-\mu < \mathrm{Re}\,\lambda < \mu$. When $x < 0$, the pole is captured by displacing the integration contour into the lower half-plane, and supplies

$$\zeta_\eta = \frac{p_0(K_0\ell)^{3/2}}{a\rho_0\omega^2}\frac{f(K_\eta)\sqrt{K_\eta^2-\mu^2}}{W_+'(-K_\eta)}(a_{00} - a_{10}K_\eta + a_{20}K_\eta^2 + K_\eta^3), \tag{4.10}$$

where $W_+' \equiv \partial W_+/\partial\lambda$. The leaky wave power $\Pi_{\rm L}$ is then given by

$$\frac{\rho_0 c_0 \Pi_{\rm L}}{|p_0|^2\ell^2} = \frac{\pi\ell|f(K_\eta)\sqrt{K_\eta^2-\mu^2}|^2}{2a\epsilon|W_+'(-K_\eta)|^2}|a_{00} - a_{10}K_\eta + a_{20}K_\eta^2 + K_\eta^3|^2\left|\frac{\partial\bar{D}}{\partial\lambda}(\lambda)\right|_{\lambda=K_\eta}, \tag{4.11}$$

where $\bar{D}(\lambda) \equiv D(\lambda K_0,\omega)/m\omega^2$ (see (2.20)).

Figure 4 illustrates the frequency dependence of the fraction $\Pi_{\rm L}/\Pi_{\rm A}$ of the total sound power radiated via the leaky wave for a steel nozzle in water for three different values of a/h. $\Pi_{\rm A}$ is calculated by numerical evaluation of the integral in (4.8 *a*). To do this we recall from figure 3*a* that the radiation directivity is relatively smooth except for the sharp spike in the leaky wave direction. An excellent numerical estimate of the non-spike contribution to the integral may therefore be obtained by using a Gaussian integration procedure on either side of the spike whose characteristic step length is larger than the spike width; the contribution from the spike is calculated from (4.11) or by integrating across the spike in the manner described in the appendix. The figure confirms the dominance of the leaky wave at very low frequencies $\omega \ll \omega_{\rm R}$ (where $\omega_{\rm R}/\omega_{\rm c} \approx 0.38, 0.038, 0.0038$, respectively, for $a/h = 10, 100, 1000$). The large narrow peak of $\Pi_{\rm L}/\Pi_{\rm A}$ occurs close to the ring frequency, where the *group velocity* of the leaky wave is small.

(d) *The acoustically compact nozzle*

Further insight into the mechanism of sound generation by source interaction with the lip can be obtained by considering the acoustically compact limit in which

$\omega a/c_0 \ll 1$. In this case, we deduce from definition (2.24) that

$$W_+(\lambda) \approx \frac{-\sqrt{1-\sigma^2}}{\alpha\mu\sqrt{A}}(\lambda + K_s)(\lambda + K_\eta), \quad \text{for } \lambda = 0(\mu). \tag{4.12}$$

Similarly, it follows from (3.6) and table 1 that only the terms in a_{00} and a_{10} need be retained in the brace brackets of (4.4). Noting also that $J_1(\kappa_0 a \sin\theta) \approx \frac{1}{2}\kappa_0 a \sin\theta$ and that $c_{10} = 1$, we then find

$$p(\boldsymbol{x}, t) \approx \frac{-\mathrm{i}p_0\ell^{3/2}(\kappa_0 a)}{2\sqrt{a}|\boldsymbol{x}|} \frac{\sin^2\theta[\cos\theta - \cos\bar{\theta}]}{(\cos\theta + \kappa_s/\kappa_0)(\cos\theta + \kappa_\eta/\kappa_0)} \mathrm{e}^{-\mathrm{i}\omega(t-|\boldsymbol{x}|/c_0)}, \quad |\boldsymbol{x}| \to \infty \tag{4.13}$$

where $\cos\bar{\theta} = -\alpha c_{00}\{12/(1-\sigma^2)\}^{1/4}$ ($\approx -1.0258\alpha$ for $a/h = 100$ and $\sigma = 0.31$).

The term in square brackets in the numerator vanishes at $\theta = \bar{\theta}$, which is close to the leaky wave angle $\theta_L = \arccos(-Re\kappa_\eta/\kappa_0) \approx \arccos(-\alpha)$. Thus, if we write,

$$p(\boldsymbol{x}, t) \approx \frac{-\mathrm{i}p_0\ell^{3/2}(\kappa_0 a)\sin^2\theta}{2\sqrt{a}|\boldsymbol{x}|(\cos\theta + \kappa_s/\kappa_0)} \left[1 - \frac{\cos\bar{\theta} + \kappa_\eta/\kappa_0}{\cos\theta + \kappa_\eta/\kappa_0}\right] \mathrm{e}^{\mathrm{i}\omega(t-|\boldsymbol{x}|/c_0)}, \tag{4.14}$$

and recall (see (D 1)) that $\kappa_s/\kappa_0 > 1$, it follows that the first term in the square brackets defines the non-singular lobe structure of the radiation field shape, and the second term is small, except at $\theta = \theta_L$ where it defines the leaky wave spike.

If the leaky wave contribution to (4.14) is discarded, the power Π_{Ao}, say, radiated in the non-singular pressure field can be computed from (4.8 *a*) to be

$$\begin{aligned}\frac{\rho_0 c_0 \Pi_{Ao}}{|p_0|^2\ell^2} &= \frac{\pi\ell(\kappa_0 a)^2}{4a}\int_0^\pi \frac{\sin^5 \mathrm{d}\theta}{(\cos\theta + \kappa_s/\kappa_0)^2} \\ &= \frac{\pi\ell(\kappa_0 a)^2}{a}\left(2(\kappa_s/\kappa_0)^2 - (\kappa_s/\kappa_0)\{(\kappa_s/\kappa_0)^2 - 1\}\ln\left[\frac{\kappa_s/\kappa_0 + 1}{\kappa_s/\kappa_0 - 1}\right] - \frac{4}{3}\right).\end{aligned} \tag{4.15}$$

At low frequencies, the ratio κ_s/κ_0 is independent of frequency (see (D 1); Smith 1987; Scott 1988; Howe 1993*c*) so that the term in the brace brackets of (4.15) does not involve the frequency, and $\rho_0 c_0 \Pi_{Ao}/|p_0|^2\ell^2$ therefore behaves like $(\omega a/c_0)^2$ at low frequencies.

The corresponding contribution Π_L from the leaky wave can be calculated by considering the limiting value of the general expression (4.11), or by substituting (4.13) into (4.8 *a*) and integrating over a small interval enclosing the leaky wave direction. In the latter case, it is easily seen that at low frequencies the integrand is small, except near $\theta = \theta_L$, and we can write

$$\frac{\rho_0 c_0 \Pi_L}{|p_0|^2\ell^2} \approx \frac{\pi\ell(k_0 a)^2 \sin^4\theta_L(\cos\theta_L - \cos\bar{\theta})^2}{4a(\cos\theta_L + \kappa_s/\kappa_0)^2}\int_0^\pi \frac{\sin\theta\,\mathrm{d}\theta}{(\cos\theta - \cos\theta_L)^2 + \{\mathrm{Im}(\kappa_\eta/\kappa_0)\}^2}. \tag{4.16}$$

When $\mathrm{Im}\{\kappa_\eta/\kappa_0\} \ll 1$, the integral is approximately equal to $\pi/\mathrm{Im}\{\kappa_\eta/\kappa_0\}$. The value of $\mathrm{Im}\{\kappa_\eta/\kappa_0\}$ can be calculated from the formula (see appendix B)

$$\mathrm{Im}\{\kappa_\eta\} \approx \frac{|\mathrm{Im}\{D(k)\}|}{|\partial D(k)/\partial k|}, \quad k = \mathrm{Re}\{\kappa_\eta\}, \tag{4.17}$$

where $D(k)$ is the dispersion function of (2.13) and, when $\omega a/c \ll 1$, $\mathrm{Re}\{\kappa_\eta\} \equiv$

$-\kappa_0 \cos\theta_L$ is well approximated as in (D 1). We accordingly find

$$\frac{\rho_0 c_0 \Pi_L}{|p_0|^2 \ell^2} \approx \frac{\pi\sigma^2}{\epsilon\sqrt{12}} \left(\frac{h}{a}\right)\left(\frac{\ell}{a}\right) \frac{\sin^4\theta_L(\cos\theta_L - \cos\bar{\theta})^2}{(\cos\theta_L + \kappa_s/\kappa_0)^2(\cos^2\theta_L - \alpha^2)^2}, \quad \omega a/c \ll 1. \tag{4.18}$$

Equations (D 1) for κ_s/κ_0 and $\cos\theta_L = -\operatorname{Re}(\kappa_\eta/\kappa_0)$ show that the right-hand side of this formula does not depend on frequency, and this confirms our earlier numerical prediction that the leaky wave is dominant at very low frequencies. In using (4.18) to make quantitative estimates, it is important to have an accurate approximation for $\cos\bar{\theta} = -\alpha c_{00}\{12/(1-\sigma^2)\}^{1/4}$; the numerical values of c_{00} given in table 2 should be used for this purpose.

The low-frequency solution (4.14) may be compared with the corresponding result for a rigid nozzle. In the compact limit, the scattered rigid nozzle pressure $p(\boldsymbol{x}, t)$ is evaluated by replacing G_p in (4.3) by the second term on the right-hand side of (3.16). This yields

$$p(\boldsymbol{x}, t) \approx \frac{-\mathrm{i}\rho_0 \ell^{3/2}(\kappa_0 a)(1-\cos\theta)}{2\sqrt{a}|\boldsymbol{x}|} \mathrm{e}^{-\mathrm{i}\omega(t-|\boldsymbol{x}|/c_0)}, \quad |\boldsymbol{x}| \to \infty. \tag{4.19}$$

This has the same order of magnitude as the non-singular component in the elastic nozzle formula (4.14). According to (D 1), $\kappa_s/\kappa_0 \approx 1$ for moderate values of a/h (not exceeding about 10 for a steel duct in water), in which case the non-singular component becomes *exactly* equal to the rigid nozzle result. This is because, when $\kappa_s/\kappa_0 \to 1$, the elastic cylinder is structurally *stiff*: the radial wavelength in the fluid of structural resonances becomes infinite and the fluid presents an infinite impedance to source-induced surface motions.

For larger values of κ_s/κ_0, the non-singular part of the elastic nozzle pressure is smaller than for the rigid duct. For example, it is about 8.4 dB smaller for a steel nozzle in water with $a/h = 100$. However, when the frequency is small enough for these estimates to be valid, the reduction in the non-singular component is more than offset by the power radiated by the leaky wave (figure 4).

(*e*) *The structural wave power*

The structural motion at large distances from the nozzle exit is dominated by a subsonic wave with radial displacement $\zeta = \zeta_s \mathrm{e}^{-\mathrm{i}(\kappa_s x + \omega t)}$, where the complex amplitude ζ_s is determined for $x \to -\infty$ by the residue contribution to the integral (4.7) from the pole just below the real axis at $\lambda = -K_s$ (where $W_+(\lambda) = 0$). The power Π_s carried by this wave (including that in the evanescent field in the fluid adjacent to the cylinder) is given formally by the formula (4.11) already used for the leaky wave, in which K_η is replaced by K_s on the right-hand side. In the subsonic region ($\omega/|\kappa_s| < c_0$), the dispersion function $\bar{D}(\lambda)$ is real. The limiting form of Π_s is easily derived at low frequencies ($\omega a/c \ll 1$) by making use of (4.12) and the representation (3.6), which leads to

$$\frac{\rho_0 c_0 \Pi_s}{p_0^2 \ell^2} \approx \frac{\pi}{\sqrt{12}\alpha\epsilon}\left(\frac{\ell}{a}\right)\left(\frac{h}{a}\right)\left(\frac{\kappa_s}{\kappa_0}\right)\left(\frac{\kappa_s^2}{\kappa_0^2} - 1\right)^2 \left(\frac{\kappa_s/\kappa_0 + \cos\bar{\theta}}{\kappa_s/\kappa_0 + \cos\theta_L}\right)^2 \times \left[\frac{\sigma^2}{(\kappa_s^2/\kappa_0^2 - \alpha^2)^2} + \frac{2\sqrt{12}\alpha\epsilon(a/h)}{(\kappa_s^2/\kappa_0^2 - 1)^2}\right]. \tag{4.20}$$

PHILOSOPHICAL TRANSACTIONS OF THE ROYAL SOCIETY A MATHEMATICAL, PHYSICAL & ENGINEERING SCIENCES

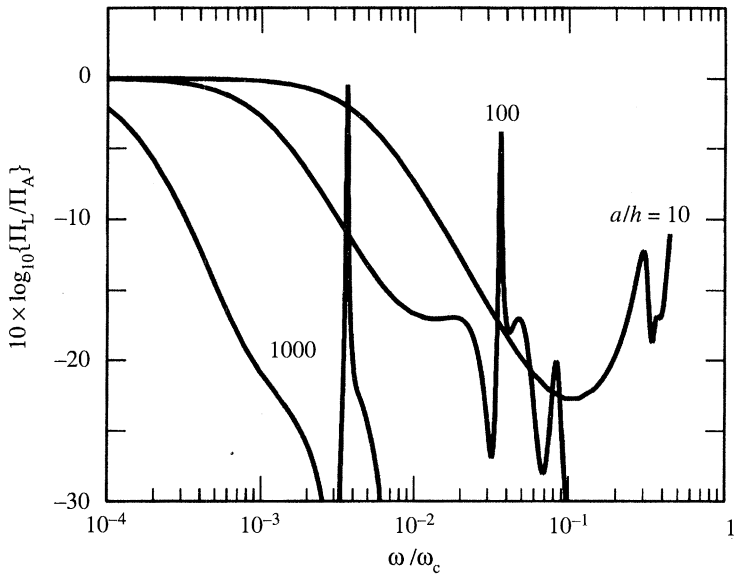

Figure 4. The fraction Π_L/Π_A of the total sound power radiated by the leaky wave for a steel nozzle in water.

The right-hand side of this result does not depend on frequency, as for the power radiated by the leaky wave. The first term in the square brackets is usually small; also $\kappa_s/\kappa_0 > 1$ (see (D 1)) and $\cos\bar{\theta} \approx cos\theta_L$. Hence, to a good approximation,

$$\frac{\rho_0 c_0 \Pi_s}{p_0^2 \ell^2} \approx 2\pi \left(\frac{\ell}{a}\right)\left(\frac{\kappa_s}{\kappa_0}\right), \quad \omega a/c \ll 1. \tag{4.21}$$

Figure 5 illustrates the frequency dependence of the ratio Π_s/Π_A of the structural to the acoustic powers for a steel duct in water for several different duct radii (Π_s is calculated for arbitrary values of ω/ω_c from (4.11) by replacing K_η by K_s). The structural power is about 10 dB or more higher than the acoustic power when $\omega < 0.1\omega_c$. As the frequency decreases further, the acoustic radiation is contained solely in the leaky mode and $\Pi_s/\Pi_A \approx \Pi_s/\Pi_L$ becomes independent of frequency. In this limit the structural power is typically 35 dB larger.

5. Noise generated by low Mach number turbulent flow from the nozzle

Consider next the production of sound by turbulence in a low Mach number nozzle flow from the elastic nozzle. Let the mean flow be at velocity U, where the Mach number $M = U/c_0 \ll 1$.

(*a*) *Formal representation of the acoustic field*

The interaction radiation will be calculated by the method used in the analysis of trailing edge noise (Chase 1972, 1975; Chandiramani 1974; Howe 1993*b*), according to which the edge generated sound is produced by the scattering of the hypothetical pressure p_I, say, that would be produced by the *same* turbulent flow if the nozzle were absent. The convection of sound waves by the low Mach number flow is neglected so that, except in the source region, the net perturbation pressure $p(\boldsymbol{x}, t)$ satisfies the

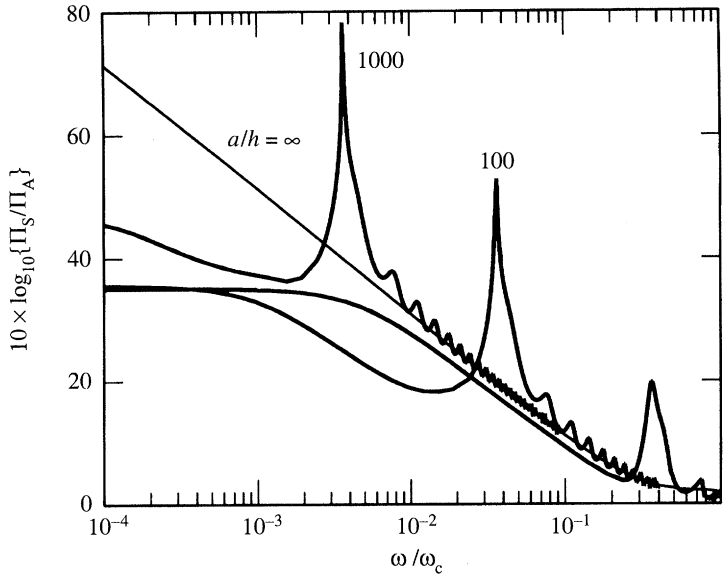

Figure 5. The ratio Π_s/Π_A of the structural and acoustic powers for a steel nozzle in water.

homogeneous wave equation

$$\left[\frac{1}{c_0^2}\frac{\partial^2}{\partial t^2}-\nabla^2\right]p=0. \tag{5.1}$$

In solving this equation, no account is taken of the influence of mean shear and turbulence, except to the extent that the latter is responsible for the pressure p_I; in particular, the scattered pressure p' is assumed to satisfy equation (5.1) everywhere.

The theory of this paper can be applied to estimate only the sound generated by the *axisymmetric* component of the turbulence pressure field p_I; it may therefore be assumed at the outset that p_I is a function of x, r and t. The scattered pressure p' will be expressed in terms of p_I and the axisymmetric Green's function $G_p(x,\bar{x},r,\bar{r},t-\tau)$ of § 2. By the usual procedure, involving the application of the divergence theorem (Morse & Ingard 1968), we can write

$$p'(\boldsymbol{x},t)=\int_{-\infty}^{\infty}\oint_S \pm\left[p'(\bar{\boldsymbol{x}},\tau)\frac{\partial}{\partial\bar{r}}G_p(x,\bar{x},r,\bar{r},t-\tau)\right.$$
$$\left.-G_p(x,\bar{x},r,\bar{r},t-\tau)\frac{\partial}{\partial\bar{r}}p'(\bar{\boldsymbol{x}},\tau)\right]\mathrm{d}S\,\mathrm{d}\tau, \tag{5.2}$$

where the surface integral is over the elastic surface S of the nozzle, the $\pm$ sign being taken, respectively, on the outer and inner surfaces of the duct.

In view of the definition of G_p, the integral on the right-hand side of equation (5.2) must vanish identically when $p'(\bar{\boldsymbol{x}},\tau)$ is replaced by $p(\bar{\boldsymbol{x}},\tau)=p_I(\bar{\boldsymbol{x}},\tau)+p'(\bar{\boldsymbol{x}},\tau)$. Since $p_I(x,a+0,t)=p_I(x,a-0,t)$, it therefore follows that (5.2) is equivalent to

$$p'(\boldsymbol{x},t)=2\pi a\int_{-\infty}^{\infty}\mathrm{d}\tau\int_{-\infty}^{0}[G_p(x,\bar{x},r,a+0,t-\tau)-G_p(x,\bar{x},r,a-0,y_3;t-\tau)]$$
$$\times\left(\frac{\partial}{\partial\bar{r}}p_i(\bar{x},\bar{r},\tau)\right)_{\bar{r}=a}\mathrm{d}\bar{x}. \tag{5.3}$$

The derivative $\partial p_{\mathrm{I}}/\partial \bar{r}$ in the integrand can be expressed in terms of $p_{\mathrm{I}}(\bar{x}, a, \tau)$ by noting that $p_{\mathrm{I}}(\boldsymbol{x}, t)$ is a solution with outgoing wave behaviour of the homogeneous equation (5.1) in the region $r > a$ exterior to the nozzle flow. It is usual, however, to express $\partial p_{\mathrm{I}}/\partial \bar{r}$ in terms of the *blocked surface pressure* p_{b}, which is the pressure that would be exerted on the interior surface of a homogeneous *rigid* duct by the same turbulent flow. When the turbulence length scale is small compared to the duct radius $p_{\mathrm{b}} \approx 2p_{\mathrm{I}}(\bar{x}, a, \tau)$, and it is easy to show that

$$\frac{\partial p_{\mathrm{I}}}{\partial \bar{r}} \approx \frac{\mathrm{i}}{2} \int_{-\infty}^{\infty} \gamma(\kappa) p_{\mathrm{b}}(\kappa, \omega') \mathrm{e}^{\mathrm{i}(\kappa \bar{x} - \omega' \tau)} \, \mathrm{d}\kappa \, \mathrm{d}\omega', \tag{5.4}$$

where

$$p_{\mathrm{b}}(\kappa, \omega') = \frac{1}{(2\pi)^2} \int_{-\infty}^{\infty} p_{\mathrm{b}}(x, t) \mathrm{e}^{-\mathrm{i}(\kappa x - \omega t)} \, \mathrm{d}x \, \mathrm{d}t. \tag{5.5}$$

To calculate the sound radiated to large distances from the nozzle, we now substitute the far field form (3.13) of Green's function, and the representation (5.4) of $\partial p_{\mathrm{I}}/\partial \bar{r}$ into the integrand of (5.3). The integration with respect to $\bar{x}$ is then easily performed, and the acoustic pressure at large distances from the nozzle found to be given by

$$\begin{aligned} p'(\boldsymbol{x}, t) \approx \frac{\mathrm{i}a \sin\theta}{2|\boldsymbol{x}|} \int_{-\infty}^{\infty} & \frac{\mu \sqrt{K_0} p_{\mathrm{b}}(\kappa, \omega) J_1(\kappa_0 a \sin\theta)}{\sqrt{\kappa} W_+(\mu \cos\theta)} \\ & \times (a_{00} + a_{10}\mu \cos\theta + a_{20}\mu^2 \cos^2\theta - \mu^3 \cos^3\theta) \\ & \times \mathrm{e}^{-\mathrm{i}\omega\{t - |\boldsymbol{x}|/c_0\}} \, \mathrm{d}\omega \, \mathrm{d}\kappa, \quad |\boldsymbol{x}| \to \infty. \end{aligned} \tag{5.6}$$

(*b*) *The acoustic pressure frequency spectrum*

The acoustic pressure spectrum $\Psi(|\boldsymbol{x}|, \theta, \omega)$ at large distance $|\boldsymbol{x}|$ in direction θ from the nozzle axis satisfies

$$\langle p'^2(\boldsymbol{x}, t) \rangle = \int_0^{\infty} \Psi(|\boldsymbol{x}|, \theta, \omega) \, \mathrm{d}\omega, \tag{5.7}$$

where the angle brackets $\langle \, \rangle$ denote an ensemble average. To express Ψ in terms of the blocked pressure p_{b}, we introduce the assumption (Chase 1972, 1974; Chandiramani 1974; Blake & Gershfeld 1989) that turbulence velocity fluctuations in the nozzle flow may be regarded as *frozen* during convection past the nozzle lip. Since we are considering only small scale turbulence (relative to the nozzle radius a), it is permissible to treat the blocked pressure as a *stationary random* function of x, the azimuthal angle ϕ and time t. For the axisymmetric pressure fluctuations, we can then write

$$\langle p_{\mathrm{b}}(\kappa, \omega) p_{\mathrm{b}}^*(\kappa', \omega') \rangle \approx \frac{1}{a} \delta(\omega - \omega') \delta(\kappa - \kappa') P_{\mathrm{b}}(\kappa, 0, \omega), \quad \kappa a \gg 1, \tag{5.8}$$

where the asterisk denotes the complex conjugate, and $P_{\mathrm{b}}(\kappa, \kappa_\perp, \omega)$ may be approximated by the *blocked pressure wavenumber–frequency spectrum* on a *plane* wall, in which the wavenumber components κ, $\kappa_\perp$ are, respectively, parallel and transverse to the mean flow direction.

Experiments at low Mach numbers reveal that $P_{\mathrm{b}}(\kappa, \kappa_\perp, \omega)$ assumes its largest values in the *convective domain* of the wavenumber plane, centred on $\kappa \approx \omega/U_{\mathrm{c}}$, $|\kappa_\perp| < U_{\mathrm{c}}/|\omega|$, where the convection velocity $U_{\mathrm{c}} \approx 0.7U$ (Chase 1980, 1987, 1991).

Corcos (1964) has proposed the following simple representation of $P_{\rm b}(\kappa,\kappa_\perp,\omega)$ in the convective region:

$$\left.\begin{aligned} P_{\rm b}(\kappa,\kappa_\perp,\omega) &= \Phi_{\rm pp}(\omega)\frac{\ell}{\pi\{1+\ell^2(\kappa-\omega/U_{\rm c})^2\}}\frac{\ell_\perp}{\pi\{1+\ell_\perp^2\kappa_\perp^2\}},\\ \ell &\approx 9U_{\rm c}/\omega, \quad \ell_\perp \approx 1.4U_{\rm c}/\omega, \end{aligned}\right\} \tag{5.9}$$

where ℓ and $\ell_\perp$ are, respectively, streamwise and spanwise turbulence correlation lengths, and $\Phi_{\rm pp}(\omega)$ is the two-sided *wall pressure frequency spectrum*, conventionally defined by $\langle p_{\rm b}^2\rangle = \int_{-\infty}^{\infty}\Phi_{\rm pp}(\omega)\,{\rm d}\omega$. This formula is applicable at low Mach numbers and $\omega\delta/U \geqslant 1$ in the immediate vicinity of the convective region, where δ is the thickness of the turbulent shear layer at the nozzle exit. Although there exist several more recent and general empirical approximations for $P_b(\kappa,\kappa_\perp,\omega)$, their use hardly alters the predicted levels of the nozzle exit noise (cf. Howe 1993*b*).

Forming the expression for $\langle p'^2(\boldsymbol{x},t)\rangle$ from representation (5.6), and using (5.8) and the definition (5.7), one finds

$$\Psi(|\boldsymbol{x}|,\theta,\omega) \approx \frac{K_0 a\mu^2|J_1(\kappa_0 a\sin\theta)|^2}{2|\boldsymbol{x}|^2|W_+(\mu\cos\theta)|^2}\sin^2\theta|a_{00}+a_{10}\mu\cos\theta+a_{20}\mu^2\cos^2\theta-\mu^3\cos^3\theta|^2 \times\int_{-\infty}^{\infty}\frac{P_{\rm b}(\kappa,0,\omega)\,{\rm d}\kappa}{|\kappa|}, \quad \omega\geqslant 0, \quad |\boldsymbol{x}|\to\infty. \tag{5.10}$$

The field shape predicted by this formula is precisely the same as that discussed in § 4 for the ring source, given in (4.8 *b*).

Because $P_{\rm b}(\kappa,0,\omega)$ is sharply peaked in the convective domain, we set $\kappa=\omega/U_{\rm c}$ in the denominator of the integrand of (5.10), and use the Corcos formula to obtain,

$$\Psi(|\boldsymbol{x}|,\theta,\omega) \approx \frac{K_0 a\mu^2|J_1(\kappa_0 a\sin\theta)|^2}{2|\boldsymbol{x}|^2|W_+(\mu\cos\theta)|^2}\sin^2\theta|a_{00}+a_{10}\mu\cos\theta+a_{20}\mu^2\cos^2\theta-\mu^3\cos^3\theta|^2 \times(U_{\rm c}\ell_\perp/\omega)\,\Phi_{\rm pp}(\omega), \quad |\boldsymbol{x}|\to\infty. \tag{5.11}$$

A similar analysis, using the axisymmetric Green's function (3.15) for a *rigid nozzle*, yields the corresponding acoustic pressure frequency spectrum:

$$\Psi_0(|\boldsymbol{x}|,\theta,\omega) \approx \frac{|J_1(\kappa_0 a\sin\theta)|^2}{2\pi|\boldsymbol{x}|^2|\bar{W}_+(\mu\cos\theta)|^2\sin^2\theta}\left(\frac{U_{\rm c}\ell_\perp}{\omega}\right)\Phi_{\rm pp}(\omega), \quad |\boldsymbol{x}|\to\infty, \tag{5.12}$$

where $\bar{W}_+(\lambda)$ is defined in (3.14).

An expression for the total sound power spectrum $\mathit{\Pi}(\omega)$ is derived from the formula $\mathit{\Pi}(\omega)=2\pi|\boldsymbol{x}|^2\int_0^\pi\Psi(|\boldsymbol{x}|,\theta,\omega)\sin\theta\,{\rm d}\theta$. A convenient non-dimensional form is

$$\frac{Uc_0\mathit{\Pi}(\omega)}{\rho_0 v_\star^4\delta_\star^3} = \frac{2\pi U|\boldsymbol{x}|^2}{(\rho_0 v_\star^2)^2\delta_\star^3}\int_0^\pi\Psi(|\boldsymbol{x}|,\theta,\omega)\sin\theta\,{\rm d}\theta, \tag{5.13}$$

where $v_\star$ is the friction velocity of the turbulent flow from the nozzle, and $\delta_\star$ is a length scale of the turbulence sources. It will be assumed that these sources are similar to those in a low Mach number turbulent boundary layer of thickness δ, and that $\delta_\star \approx \frac{1}{8}\delta$ is the boundary layer displacement thickness. We can then use the empirical approximation (due to Chase (1980))

$$\frac{(U/\delta_\star)\,\Phi_{\rm pp}(\omega)}{(\rho_0 v_\star^2)^2} \approx \frac{(\omega\delta_\star/U)^2}{[(\omega\delta_\star/U)^2+\alpha_{\rm p}^2]^{3/2}}, \quad \alpha_{\rm p}=0.12, \quad \omega\delta_\star/U\geqslant 0.1, \tag{5.14}$$

in terms of which the elastic and rigid nozzle acoustic pressure spectra $\Pi(\omega)$ and $\Pi_0(\omega)$ are given, respectively, by

$$\frac{Uc_0\Pi(\omega)}{\rho_0 v_\star^4 \delta_\star^3} = \frac{1.4(U_c/U)^2}{[(\omega\delta_\star/U)^2+\alpha_p^2]^{3/2}} \int_0^\pi \frac{K_0 a\mu^2 \sin^3\theta |J_1(\kappa_0 a\sin\theta)|^2}{|W_+(\mu\cos\theta)|^2} \times |a_{00}+a_{10}\mu\cos\theta+a_{20}\mu^2\cos^2\theta-\mu^3\cos^3\theta|\,\mathrm{d}\theta, \tag{5.15}$$

$$\frac{Uc_0\Pi(\omega)}{\rho_0 v_\star^4 \delta_\star^3} = \frac{1.4(U_c/U)^2}{[(\omega\delta_\star/U)^2+\alpha_p^2]^{3/2}} \int_0^\pi \frac{(1-\cos\theta)^2 |J_1(\kappa_0 a\sin\theta)|^2}{\sin\theta |\bar{W}_+(\mu\cos\theta)|^2}. \tag{5.16}$$

Recall that, in order to apply these formulae to examine the influence of nozzle elasticity on the acoustic power, it is necessary for the length scale of the turbulence motions to be small relative to both the structural wavelengths and the nozzle radius. The characteristic wavenumber of the turbulence sources $\sim \omega/U_c$, and the first condition is therefore equivalent to (3.1) with $\Lambda \equiv (\omega/U_c)/K_0$. The second requires $\omega a/U_c \gg 1$. Expressing both conditions in terms of the non-dimensional frequency ω/ω_c, they are seen to require, respectively, that

$$\frac{\omega}{\omega_c} \gg \frac{M_c\sqrt{h/a}}{\alpha 12^{1/4}}, \quad \frac{\omega}{\omega_c} \gg \frac{M_c h/a}{\alpha 12^{1/2}}, \quad M_c = U_c/c_0. \tag{5.17}$$

For steel in water, these conditions are satisfied provided $\omega/\omega_c \gg 2M_c\sqrt{h/a}$.

In figure 6, the predicted total sound power spectra $\Pi(\omega)$ (solid curves) and $\Pi_0(\omega)$ (dotted) for steel and rigid nozzles in water for $\delta_\star/a = 0.1, 0.01, 0.005$ are plotted, and

$$M = U/c_0 = 0.01, \quad a/h = 100.$$

As $\omega/\omega_c \to 0$, all three elastic predictions become equal; this is because the integrand of (5.15), which essentially measures the *efficiency* of the nozzle-based sources, does not depend on frequency at low frequencies, when most of the sound is radiated via leaky extensional waves. The steep troughs in $\Pi(\omega)$ for $\delta_\star/a = 0.01$ and 0.005 occur at the ring frequency $\omega_R/\omega_c = 0.038$, i.e. since

$$\omega\delta_\star/U \equiv \frac{\alpha\sqrt{12}}{M}(\omega/\omega_c)(a/h)(\delta_\star/a), \tag{5.18}$$

at $\omega\delta_\star/U \approx 3.6$ and 1.3, respectively. The same trough occurs at $\omega\delta_\star/U \approx 36$ when $\delta_\star/a = 0.1$. At frequencies exceeding the ring frequency the elastic nozzle power is below the corresponding rigid nozzle prediction, but they ultimately become equal when $\omega/\omega_c \to 1$ (as in the case of the elastic trailing edge noise for a flat elastic surface (Howe 1993*b*)). The elastic nozzle results for $\delta_\star/a = 0.1$ must be treated with caution, since condition (5.17) is violated in this case when $\omega\delta_\star/U < 1$ ($\omega/\omega_c < 0.001$). The predictions for $\delta_\star/a = 0.01, 0.005$ should be valid down to $\omega\delta_\star/U = 0.1$, however, and indicate that surface compliance produces only a marginal decrease in the acoustic sound power. Thus, although structural compliance would normally be expected to reduce the intensity of the directly scattered sound, the effect is offset at lower frequencies by the excitation of leaky waves, to the extent that the elastic nozzle sound power is typically only 2 or 3 dB smaller than that produced by the same flow from a rigid nozzle. On the other hand, the dominance of leaky waves at low frequencies implies that the radiation directivity will tend to be sharply peaked (at about 106° to the mean flow direction) for the elastic nozzle (cf. figure 3).

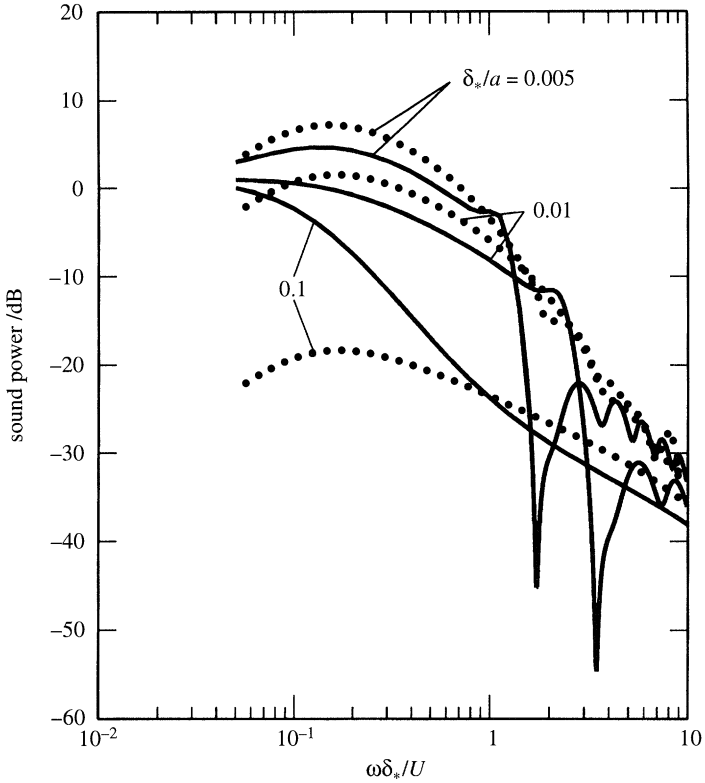

Figure 6. Sound power spectra of the axisymmetric component of the noise generated by turbulent shear flow from circular cylindrical nozzle for $\delta_\star/a = 0.1$, 0.01 and 0.005: —, steel nozzle in water; • • •, rigid nozzle.

It should also be remembered that, according to figure 5, the power scattered into subsonic structural modes is typically 20 dB or more larger than that directly radiated from the nozzle exit. Any practical estimate of the net power radiated into the fluid should therefore take account of additional sound produced by the secondary scattering of this structural energy.

6. Conclusions

In low Mach number flows, the intensity of sound generated by turbulence near solid structures is generally determined by the unsteady flow-induced surface forces. The largest surface forces usually occur when the body is *rigid*, when they cannot be relieved by compensatory motion of the surface. The introduction of structural compliance would therefore be expected to lead to a reduction in the intensity of the radiated sound. This conclusion is supported by theoretical analyses of turbulence interacting with acoustically compact bodies, and for trailing edge noise, where the edge is modelled by a thin elastic half-plane (Crighton & Leppington 1970; Howe 1993*b*, *d*). However, most structures exhibit a spectrum of resonant responses that permit the body to absorb substantial amounts of flow energy that is subsequently converted into sound when the resonant mode interacts with structural irregularities. Thus, in the trailing edge noise problem, the direct radiation from the edge is greatly

reduced compared to that from a rigid edge in the same turbulent flow; but the structural power generated at the edge is typically 20 dB or more higher than the directly radiated edge noise, and the subsequent scattering of structural modes may actually cause the overall noise levels to be increased relative to the rigid edge.

The investigation described in this paper, of the sound generated by sources in the vicinity of an elastic nozzle, is an example of a structure in which both of the above mechanisms are important. First, the reaction of the elastic surface to forcing by the turbulence generally results in a corresponding reduction, relative to a rigid nozzle, in the acoustic intensity in most directions of propagation. The fluid-structure interaction also generates both extensional and flexural waves in the duct wall, that propagate upstream from the nozzle exit. The extensional waves are *leaky*, they have supersonic phase velocity and are weakly coupled through the effect of surface curvature to radial wall motions. This causes structural energy to be radiated into the fluid, producing an intense beam of sound in a direction determined by the ratio of the acoustic and extensional wave phase speeds (for a steel nozzle in water the direction makes an angle of about 106° with the nozzle axis). As the frequency decreases below the ring frequency of the duct the acoustic radiation tends to be dominated by the leaky waves, and, ultimately, at very low frequencies all of the sound is radiated by this means. The flexural waves generated at the nozzle have subsonic phase velocities and are analogous to the bending waves produced by turbulence near the edge of a thin elastic plate. Their power is typically 30–40 dB greater than the leaky wave power, and they are a potentially important additional source of sound when scattering occurs.

The application of the theory to study the noise generated by low Mach number turbulent flow from a steel nozzle in water indicates that the overall effect of surface compliance is to reduce the direct radiation from the nozzle (relative to that produced by the same flow from a rigid nozzle) by about 3 dB. At low frequencies (below the ring frequency of the duct), the excitation of leaky extensional modes ensures that the elastic noise levels do not fall significantly below those for the rigid nozzle. Indeed, whereas the conventional aerodynamic source efficiency varies like M^3 at low turbulence Mach numbers M (Curle 1955), the efficiency of sound generation by the leaky waves varies linearly with M, and this counteracts the low frequency fall off in acoustic intensity that would otherwise be caused by surface compliance.

This work was sponsored by the Applied Hydrodynamics Research Program of the Office of Navel Research under grant N00014-93-1-0111, administered by Mr James A. Fein. It is a pleasure to acknowledge the benefit of discussions with Dr M. M. Sevik during the preparation of the paper.

Appendix A. Formulation of the leaky wave problem

We consider the sound radiated into the region $x_2 > 0$ of the rectangular coordinate system (x_1, x_2, x_3) by a leaky wave established on a linear conservative elastic surface $x_2 = 0$. Denote by ζ the surface displacement in the positive x_2-direction, and let the leaky wave be generated in the vicinity of $x_1 = 0$, propagate parallel to the positive x_1-axis and be given by

$$\zeta = \zeta_0 \mathrm{e}^{\mathrm{i}(\kappa x_1 - \omega t)}, \quad \omega > 0, \tag{A 1}$$

where only the real part of the right-hand side is to be taken. The complex surface wavenumber

$$\kappa = \kappa_{\mathrm{R}} + \mathrm{i}\kappa_{\mathrm{I}}, \quad \kappa_{\mathrm{R}}, \kappa_{\mathrm{I}} > 0, \tag{A 2}$$

where $\kappa_{\mathrm{I}} \ll \kappa_{\mathrm{R}}$.

Let the equation describing time harmonic waves on the elastic surface propagating parallel to the x_1-axis be taken in the form

$$H(-\mathrm{i}\partial/\partial x_1,\omega)\zeta = -p, \tag{A 3}$$

where p is the fluid pressure on $x_2 = +0$ and H is a linear operator. The pressure satisfies the acoustic equation in $x_2 > 0$, and p and ζ are also related by $\rho_0\omega^2\zeta = \partial p/\partial x_2$ on $x_2 = 0$. The general solution of these equations representing outgoing waves can be cast in the form

$$\zeta = \int_{-\infty}^{\infty} \frac{F(k,\omega)}{D(k,\omega)} \mathrm{e}^{\mathrm{i}kx_1}\,\mathrm{d}k, \quad p = -\mathrm{i}\rho_0\omega^2 \int_{-\infty}^{\infty} \frac{F(k,\omega)}{\gamma(k)D(k,\omega)} \mathrm{e}^{\mathrm{i}\{kx_1+\gamma(k)x_2\}}\,\mathrm{d}k, \quad x_2 > 0, \tag{A 4}$$

where the time factor $\mathrm{e}^{-\mathrm{i}\omega t}$ is temporarily suppressed, $F(k,\omega)$ is a smoothly varying function characterizing the source of the motion and $D(k,\omega)$ is the dispersion function

$$D(k,\omega) \equiv H(k,\omega) - \mathrm{i}\rho_0\omega^2/\gamma(k). \tag{A 5}$$

For a conservative elastic system, $H(k,\omega)$ is real for real values of k. The leaky wavenumber κ satisfies $D(\kappa,\omega) = 0$ and lies close to the acoustic interval of the real k-axis, i.e. $0 < \kappa_\mathrm{R} < \kappa_0$, $0 < \kappa_\mathrm{I} \ll \kappa_0$.

We shall show that the acoustic power radiated by the leaky wave (per unit length in the x_3-direction) is given by

$$\Pi_\mathrm{L} = \frac{\omega}{4}|\zeta_0|^2 \left|\frac{\partial D}{\partial k}(k,\omega)\right|_{k=\kappa_\mathrm{R}}. \tag{A 6}$$

This is a generalization of the formula for the power transmitted by an *evanescent* wave, whose amplitude decreases exponentially with distance x_2 from the surface. In that case, however, $\kappa_\mathrm{R} > \kappa_0$, $\kappa_\mathrm{I} \equiv 0$ (in the absence of structural damping) and $\partial D(k,\omega)/\partial k$ is real at $k = \kappa$. There is no requirement that conditions on $x_2 = 0$ are homogeneous. The formula is applicable, for example, to a diffraction problem involving surface irregularities, etc., provided the solution can be cast in the form (A 4). The axisymmetric formula (4.9) may be obtained by multiplying (A 6) by the circumference $2\pi a$ of the cylinder or by an obvious modification of the argument outlined below.

Appendix B. Proof of (4.17)

We first derive approximation (4.17), which expresses κ_I in terms of κ_R.

Expand $D(\kappa,\omega) \equiv D(\kappa_\mathrm{R} + \mathrm{i}\kappa_\mathrm{I},\omega) = 0$ to first order in κ_I to obtain $\kappa_\mathrm{I} \approx \mathrm{i}D(\kappa_\mathrm{R},\omega)/D'(\kappa_\mathrm{R},\omega)$, where $D' = \partial D/\partial k$. Since $\kappa_\mathrm{I} > 0$, it follows that, if $D(\kappa_\mathrm{R},\omega) = |D(\kappa_\mathrm{R},\omega)|\mathrm{e}^{\mathrm{i}\varphi}$, then $D'(\kappa_\mathrm{R},\omega) = |D'(\kappa_\mathrm{R},\omega)|\mathrm{e}^{\mathrm{i}(\varphi+\pi/2)}$, and therefore that

$$\kappa_\mathrm{I} \approx |D(\kappa_\mathrm{R},\omega)|/|D'(\kappa_\mathrm{R},\omega)|. \tag{B 1}$$

Let $D(k,\omega) \equiv D_\mathrm{R}(k,\omega) + \mathrm{i}D_\mathrm{I}(k,\omega)$, where D_R and D_I are the respective real and imaginary parts of D. Then

$$D_\mathrm{R}(\kappa_\mathrm{R},\omega) \approx \kappa_\mathrm{I}D_\mathrm{I}'(\kappa_\mathrm{R},\omega), \quad D_\mathrm{I}(\kappa_\mathrm{R},\omega) \approx -\kappa_\mathrm{I}D_\mathrm{R}'(\kappa_\mathrm{R},\omega),$$

where the primes again denote differentiation with respect to k. Equation (4.17)

now follows from (B 1) by observing that $D_{\mathrm{R}}(\kappa_{\mathrm{R}},\omega)$ is a second-order quantity, because $D'_{\mathrm{I}}(\kappa_{\mathrm{R}},\omega)$ must vanish identically in the absence of fluid loading. For the two-dimensional problem of appendix A, we have

$$\kappa_{\mathrm{I}} \approx \frac{|D_{\mathrm{I}}(\kappa_{\mathrm{R}},\omega)|}{|D'(\kappa_{\mathrm{R}},\omega)|} = \frac{\rho_0\omega^2/\gamma(\kappa_{\mathrm{R}})}{|D'(\kappa_{\mathrm{R}},\omega)|}. \tag{B 2}$$

Appendix C. Proof of (A 6)

The power $\mathit{\Pi}$ radiated into $x_2 > 0$ per unit distance in x_3 can be calculated from the formula $\mathit{\Pi} = \int_{-\infty}^{\infty}\langle pv\rangle\,\mathrm{d}x_1$, where $v = \mathrm{Re}\{-\mathrm{i}\omega\zeta\}$ is the normal velocity on $x_2 = 0$, and the angle brackets denote an average over a wave period. Using the Fourier integral representations (A 4), with the time factor $\mathrm{e}^{-\mathrm{i}\omega t}$ restored, we find

$$\mathit{\Pi} = \pi\rho_0\omega^3\int_{-\kappa_0}^{\kappa_0}\frac{|F(k,\omega)|^2}{\gamma(k)|D(k,\omega)|^2}\,\mathrm{d}k. \tag{C 1}$$

When the leaky wave pole at $k = \kappa$ approaches the real axis, the integrand has a very large peak at $k = \kappa_{\mathrm{R}}$, in the neighbourhood of which $|D(k,\omega)|^2 \approx |D'(\kappa,\omega)|^2\{(k-\kappa_{\mathrm{R}})^2 + \kappa_{\mathrm{I}}^2\}$. When $\kappa_{\mathrm{I}} \ll \kappa_0$, the contribution $\mathit{\Pi}_{\mathrm{L}}$ to the integral from the immediate vicinity of the leaky wave pole is therefore given by

$$\mathit{\Pi}_{\mathrm{L}} \approx \frac{\pi\rho_0\omega^3|F(\kappa_{\mathrm{R}},\omega)|^2}{\gamma(\kappa_{\mathrm{R}})|D'(\kappa,\omega)|^2}\int_{-\infty}^{\infty}\frac{\mathrm{d}k}{\{(k-\kappa_{\mathrm{R}})^2+\kappa_{\mathrm{I}}^2\}} = \frac{\pi^2\rho_0\omega^3|F(\kappa_{\mathrm{R}},\omega)|^2}{\kappa_{\mathrm{I}}\gamma(\kappa_{\mathrm{R}})|D'(\kappa,\omega)|^2}. \tag{C 2}$$

The surface displacement due to the leaky wave is determined by the residue contribution to the first integral of (A 4) from the pole at $k = \kappa$, just above the real axis, from which the complex amplitude at $x = 0$ is found to be

$$\zeta_0 = 2\pi\mathrm{i}\frac{F(\kappa,\omega)}{D'(\kappa,\omega)}. \tag{C 3}$$

Equation (A 6) is now obtained by approximating the smoothly varying source function $F(\kappa,\omega)$ in (C 3) by $F(\kappa_{\mathrm{R}},\omega)$, and substituting into (C 2) for κ_{I} from (B 2) and for $F(\kappa_{\mathrm{R}},\omega)/D'(\kappa,\omega)$ from (C 3).

Appendix D. Asymptotic approximations for the leaky and structural wavenumbers

At low frequencies

$$\left.\begin{aligned}
\mathrm{Re}\{\kappa_\eta/\kappa_0\} &\approx \frac{\alpha\sqrt{2}[\beta + (\sigma^2-\alpha^2)/(1-\sigma^2)]^{1/2}}{[\beta + \sqrt{(\beta-2\alpha^2)^2 - 4\alpha^2\sigma^2(1-\alpha^2)/(1-\sigma^2)}]^{1/2}},\\
\mathrm{Im}\{\kappa_\eta/\kappa_0\} &\approx \frac{\pi\sqrt{3}\epsilon}{2\sigma^2}\left(\frac{a}{h}\right)\mu(\kappa_0 a)^2(\cos^2\theta_{\mathrm{L}} - \alpha^2)^2, \quad \cos\theta_{\mathrm{L}} = -\,\mathrm{Re}\{\kappa_\eta/\kappa_0\},\\
\kappa_{\mathrm{s}} &\approx \kappa_0\sqrt{\beta},\\
\beta &= 1 + \frac{\alpha^2}{(1-\sigma^2)}\left(1 + 2\frac{\rho_0 a}{\rho_{\mathrm{s}} h}\right), \quad \omega a/c \ll 1.
\end{aligned}\right\} \tag{D 1}$$

Table 2. *The variable coefficients c_{in} for steel in water*

$\log_{10}(a/h)$	$c_{00}, -c_{02}, c_{22}$	c_{01}
1.0	0.548 076	−0.775 096i
1.2	0.546 690	−0.773 137i
1.4	0.544 860	−0.770 549i
1.6	0.542 607	−0.767 362i
1.8	0.540 052	−0.763 749i
2.0	0.537 395	−0.759 992i
2.2	0.534 855	−0.756 399i
2.4	0.532 595	−0.753 202i
2.6	0.530 694	−0.750 515i
2.8	0.529 161	−0.748 347i
3.0	0.527 957	−0.746 643i

Appendix E. Supplement to table 1 for steel in water

Six-figure approximations for the coefficients c_{in} of table 1 are given in table 2 for a range of values of a/h for a steel nozzle in water.

References

Abramowitz, M. & Stegun, I. A. (eds) 1970 *Handbook of Mathematical Functions (US Dept. of Commerce, Nat. Bur. Stands. Appl. Math. Ser. 55)* 9th corrected printing.

Amiet, R. K. 1975 Acoustic radiation from an airfoil in a turbulent stream. *J. Sound Vib.* **41**, 407–420.

Amiet, R. K. 1976 Noise due to turbulent flow past a trailing edge. *J. Sound Vib.* **47**, 387–393.

Amiet, R. K. 1986 Airfoil gust response and the sound produced by airfoil-vortex interaction. *J. Sound Vib.* **107**, 487–506.

Blake, W. K. & Gershfeld, J. L. 1989 The aeroacoustics of trailing edges. In *Frontiers in experimental fluid mechanics (Lecture Notes in Engineering 46)* (ed. M. Gad-el-Hak).

Born, M. & Wolf, E. 1975 *Principles of optics*, 5th edn. Oxford: Pergamon.

Cannell, P. & Ffowcs Williams, J. E. 1973 Radiation from line vortex filaments exhausting from a two-dimensional semi-infinite duct. *J. Fluid Mech.* **58**, 65–80.

Cannell, P. A. 1975 Edge scattering of aerodynamic sound by a lightly loaded elastic half-plane. *Proc. R. Soc. Lond.* A **347**, 213–238.

Cannell, P. A. 1976 Acoustic edge scattering by a heavily loaded elastic half-plane. *Proc. R. Soc. Lond.* A **350**, 71–89.

Chase, D. M. 1972 Sound radiated by turbulent flow off a rigid half-plane as obtained from a wavevector spectrum of hydrodynamic pressure. *J. Acoust. Soc. Am.* **52**, 1011–1023.

Chase, D. M. 1975 Noise radiated from an edge in turbulent flow. *AIAA Jl* **13**, 1041–1047.

Chase, D. M. 1980 Modeling the wavevector-frequency spectrum of turbulent boundary layer wall pressure. *J. Sound Vib.* **70**, 29–67.

Chase, D. M. 1987 The character of the turbulent wall pressure spectrum at subconvective wavenumbers and a suggested comprehensive model. *J. Sound Vib.* **112**, 125–147.

Chase, D. M. 1991 The wave-vector-frequency spectrum of pressure on a smooth plane in turbulent boundary-layer flow at low Mach number. *J. Acoust. Soc. Am.* **90**, 1032–1041.

Chandiramani, K. L. 1974 Diffraction of evanescent waves, with applications to aerodynamically scattered sound and radiation from unbaffled plates. *J. Acoust. Soc. Am.* **55**, 19–29.

Corcos, G. M. 1964 The structure of the turbulent pressure field in boundary layer flows. *J. Fluid Mech.* **18**, 353–378.

Cremer, L., Heckl, M. & Ungar, E. E. 1988 *Structure-borne sound*, 2nd edn. New York: Springer.

Crighton, D. G. 1972*a* The excess noise field of subsonic jets. ARC Noise Research Comm. Paper ARC 33 714.

Crighton, D. G. 1972*b* Radiation from vortex filament motion near a half plane. *J. Fluid Mech.* **51**, 357–362.

Crighton, D. G. 1972*c* Acoustic edge scattering of elastic surface waves. *J. Sound Vib.* **22**, 25–32.

Crighton, D. G. 1975 Scattering and diffraction of sound by moving bodies. *J. Fluid Mech.* **72**, 209–227.

Crighton, D. G. 1984 Long-range acoustic scattering by surface inhomogeneities beneath a turbulent boundary layer. *J. Vib. Stress Reliabilty Design* **106**, 376–382.

Crighton, D. G. 1989 The 1988 Rayleigh Medal lecture: fluid loading—the interaction between sound and vibration. *J. Sound Vib.* **133**, 1–27.

Crighton, D. G. 1991 Airframe noise. In *Noise sources (Aeroacoustics of flight vehicles: theory and practice 1)* (ed. H. H. Hubbard), ch. 7, NASA ref. pub. no. 1258

Crighton, D. G. & Leppington, F. G. 1970 Scattering of aerodynamic noise by a semi-infinite compliant plate. *J. Fluid Mech.* **43**, 721–736.

Crighton, D. G. & Leppington, F. G. 1971 On the scattering of aerodynamic noise. *J. Fluid Mech.* **46**, 577–597.

Crow, S. C. & Champagne, F. H. 1971 Orderly structure in jet turbulence. *J. Fluid Mech.* **48**, 547–591.

Curle, N. 1955 The influence of solid boundaries upon aerodynamic sound. *Proc. R. Soc. Lond.* A **231**, 505–514.

Ffowcs Williams, J. E. & Hall, L. H. 1970 Aerodynamic sound generation by turbulent flow in the vicinity of a scattering half-plane. *J. Fluid Mech.* **40**, 657–670.

Goldstein, M. 1974 Unified approach to aerodynamic sound generation in the presence of solid boundaries. *J. Acoust. Soc. Am.* **56**, 497–509.

Graff, K. F. 1975 *Wave motion in elastic solids.* Columbus, OH: Ohio State University Press.

Hinze, J. O. 1975 *Turbulence*, 2nd edn. New York: McGraw-Hill.

Howe, M. S. 1975 Contributions to the theory of aerodynamic sound, with application to excess jet noise and the theory of the flute. *J. Fluid Mech.* **71**, 625–673.

Howe, M. S. 1992 Sound produced by an aerodynamic source adjacent to a partly coated, finite elastic plate. *Proc. R. Soc. Lond.* A **436**, 351–372.

Howe, M. S. 1993*a* The compact Green's function for the semi-infinite elastic plate, with application to trailing edge noise and blade-vortex interaction noise. *J. Acoust. Soc. Am.* **94**, 2353–2364.

Howe, M. S. 1993*b* Structural and acoustic noise produced by turbulent flow over an elastic trailing edge. *Proc. R. Soc. Lond.* A **444**, 533–554.

Howe, M. S. 1993*c* On the sound produced when flexural waves are reflected at the open end of a fluid loaded elastic cylinder. *J. Acoust. Soc. Am.* **96**, 265–276.

Howe, M. S. 1993*d* Elastic blade-vortex interaction noise. *J. Sound Vib.* **177**, 325–337.

Jones, D. S. 1964 *The theory of electromagnetism.* Oxford: Pergamon Press.

Jones, D. S. 1982 *The theory of generalised functions*, 2nd edn. Cambridge University Press.

Kambe, T., Minota, T. & Ikushima, Y. 1985 acoustic wave emitted by a vortex ring passing near the edge of a half-plane. *J. Fluid Mech.* **155**, 77–103.

Kraus, H. 1967 *Thin elastic shells.* New York: Wiley.

Landau, L. D. & Lifshitz, E. M. 1987 *Fluid mechanics*, 2nd edn. Oxford: Pergamon.

Lawrie, J. B. 1986 Vibrations of a heavily loaded, semi-infinite, cylindrical elastic shell. I. *Proc. R. Soc. Lond.* A **408**, 103–128.

Lawrie, J. B. 1987 Vibrations of a heavily loaded, semi-infinite, cylindrical elastic shell. II. *Proc. R. Soc. Lond.* A **414**, 371–387.

PHILOSOPHICAL TRANSACTIONS OF THE ROYAL SOCIETY A MATHEMATICAL, PHYSICAL & ENGINEERING SCIENCES

Leppington, F. G. 1971 Scattering of quadrupole sources near the end of a rigid semi-infinite circular pipe. Report of the ARC Working Party on novel aerodynamic noise source mechanisms at low jet speeds, ch. 5, ARC 32 925 N.742.

Lighthill, M. J. 1958 *An introduction to Fourier analysis and generalised functions.* Cambridge University Press.

Lilley, G. M. 1991 Jet noise classical theory and experiments. In *Noise Sources (Aeroacoustic of flight vehicles: theory and practice 1)* (ed. H. H. Hubbard), ch. 4, NASA ref. publ. 1258.

Maestrello, L., Frendi, A. & Brown, D. E. 1992 Nonlinear vibration and radiation from a panel with transition to chaos. *AIAA Jl* **30**, 2632–2638.

Morse P. M. & Ingard, K. U. 1968 *Theoretical acoustics.* New York: McGraw-Hill.

Nayak, P. R. 1970 Line admittance of infinite isotropic fluid loaded plates. *J. Acoust. Soc. Am.* **47**, 191–201 (Errata 1970 *J. Acoust. Soc. Am.* **49**, 380).

Powell, A. 1977*a* Flow noise: a perspective on some aspects of flow noise, and of jet noise in particular: Part 1. *Noise Con. Eng.* **8**, 69–80.

Powell, A. 1977*b* Flow noise: a perspective on some aspects of flow noise, and of jet noise in particular: Part 2. *Noise Con. Eng.* **8**, 108–119.

Ribner, H. S. 1981 Perspectives on jet noise. AIAA paper 81-0428.

Scott, J. F. M. 1988 The free modes of propagation of an infinite fluid-loaded thin cylindrical shell. *J. Sound Vib.* **125**, 241–280.

Smith Jr, P. W. 1987 Scatter of axisymmetric surface waves from an obstacle in a thin cylindrical shell. Bolt Beranek and Newman Tech. Memo. 978.

Watson, G. N. 1944 *A treatise on the theory of Bessel functions*, 2nd edn. Cambridge University Press.

Received 20 September 1993; revised 9 August 1994; accepted 8 November 1994

PHILOSOPHICAL TRANSACTIONS OF THE ROYAL SOCIETY A MATHEMATICAL, PHYSICAL & ENGINEERING SCIENCES